The University of Oklahoma

OKHEP-05-01
hep-ph/yymmnnn
October, 2007

SUSY QCD Corrections to Higgs Pair Production from Bottom Quark Fusion

Sally Dawson[a], Chung Kao[b], Yili Wang[b]

[a] *Department of Physics,*
Brookhaven National Laboratory,
Upton, NY 11973, USA
[b] *Homer L. Dodge Department of Physics and Astronomy,*
University of Oklahoma
Norman, Oklahoma 73019, USA

arXiv:0710.4331v1 [hep-ph] 23 Oct 2007

Abstract

We present a complete next-to-leading order (NLO) calculation for the total cross section for inclusive Higgs pair production via bottom-quark fusion at the CERN Large Hadron Collider (LHC) in the minimal supersymmetric standard model (MSSM) and the minimal supergravity model (mSUGRA). We emphasize the contributions of squark and gluino loops (SQCD) and the decoupling properties of our results for heavy squark and gluino masses. The enhanced couplings of the b quark to the Higgs bosons in supersymmetric models with large $\tan\beta$ yield large NLO SQCD corrections in some regions of parameter space.

I. INTRODUCTION

In the standard model (SM), only one Higgs doublet is introduced and one neutral Higgs boson remains after electroweak symmetry breaking. In the Minimal Supersymmetric Standard Model (MSSM) [1], two Higgs doublets are required to break the electroweak symmetry. The two Higgs doublets, ϕ_1 and ϕ_2, couple to fermions with weak isospin $-1/2$ and $+1/2$ respectively [2]. After spontaneous symmetry breaking, there remain five physical Higgs bosons: a singly charged Higgs boson $H^{\pm}$, two neutral CP-even scalars h and H, and a neutral CP-odd pseudoscalar A. The Higgs potential is constrained by supersymmetry such that all tree-level Higgs boson masses and couplings are determined by just two independent parameters, commonly chosen to be the mass of the CP-odd pseudoscalar (M_A) and the ratio of vacuum expectation values of the neutral Higgs fields ($\tan\beta \equiv v_2/v_1$).

In the standard model, gluon fusion is the dominant process for producing a pair of Higgs bosons via triangle and box diagrams with internal top quarks and bottom quarks [3, 4, 5, 6, 7, 8, 9]. The Yukawa coupling of the Higgs boson to bottom quarks in the standard model is proportional to m_b/v_{SM}, where v_{SM} is the vacuum-expectation value of the Higgs field, and is hence very weak. Thus, at the Fermilab Tevatron and CERN Large Hadron Collider(LHC), the rate for inclusive Higgs pair production from b quark fusion is small [8, 10]. However, it can become significant in supersymmetric models with large $\tan\beta$ since the Yukawa couplings of the Higgs bosons to the b quark are enhanced by $1/\cos\beta$. In the Minimal Supersymmetric Model (MSSM), the production rate of pairs of the lightest neutral Higgs boson (hh) from $b\overline{b}$ fusion is larger than the rate from the gluon-gluon initial state for $\tan\beta \leq 35$ and moderate values of M_A ($M_A \sim 300\ GeV$), while the rate for pair production of the heavier neutral Higgs bosons (HH and AA) from $b\overline{b}$ fusion is highly suppressed relative to the gluon-gluon production mechanism at small $\tan\beta$[8, 11]. This makes it of interest to evaluate higher order corrections to the rates.

One of the most powerful ways to distinguish between the Higgs boson of the standard model and those of the MSSM is to measure the trilinear neutral Higgs boson couplings. This measurement is extremely challenging in most scenarios [12, 13, 14, 15, 16]. The enhanced Higgs pair production rates from bottom quark fusion when $\tan\beta$ is large provide discovery potential for determining the trilinear Higgs couplings in the MSSM. The rate for Higgs boson production from bottom quark fusion[17] has been computed to NNLO[18] and the electroweak and SUSY QCD corrections included to one-loop[19]. Also, the rate for Higgs production in association with a b quark has been computed to NLO[20, 21, 22, 23, 24, 25] including SUSY QCD corrections[26].

In this paper, we present a complete next-to-leading order (NLO) SUSY QCD calculation for Higgs pair production via bottom quark fusion. The leading order (LO) process is $b\overline{b} \to \phi\phi$ (where $\phi = h, H, A$) and the NLO cross section includes both $\mathcal{O}(\alpha_s)$ and $\mathcal{O}(1/\Lambda)$ corrections, where $\Lambda \equiv \ln(M_\phi/m_b)$ [27, 28, 29, 30]. The subprocess $bg \to b\phi\phi$ contributes $\mathcal{O}(1/\Lambda)$ corrections to the leading order cross section for $b\overline{b} \to \phi\phi$. Theoretical predictions depend on the number of b quarks tagged. Here, we consider only inclusive processes in which there are no tagged b quarks. The NLO pure QCD corrections have been computed in Ref. [10]. The focus of this work is the inclusion of the $\mathcal{O}(\alpha_s)$ SUSY QCD (SQCD) corrections, which consist of squark and gluino loop contributions. We also present a detailed study of the effects of the SUSY parameters on the production rate in the MSSM and mSUGRA models.

In section II, we review the leading-order cross section for $pp \to \phi\phi$ from $b\bar{b}$ fusion. In

section III, we provide the complete next-to-leading order (NLO) SQCD corrections from gluino and squark loops for $b\bar{b} \to \phi\phi$ production. Numerical results are given in Section IV and conclusions are drawn in Section V. In addition, there are three Appendices. Appendix A defines the scalar integrals [31, 32, 33, 34] used in our computation, Appendix B contains the coefficients used in computing the virtual SQCD corrections and Appendix C presents the Yukawa couplings, Higgs trilinear couplings and Higgs-squark-squark couplings in the MSSM.

II. LOWEST ORDER PRODUCTION IN $b\bar{b} \to \phi\phi$

The leading order (LO) inclusive cross section for $pp \to \phi\phi$ via $b\bar{b} \to \phi\phi$ is

$$\sigma_{LO} = \int dx_1 dx_2 \left[b(x_1)\bar{b}(x_2) + \bar{b}(x_1)b(x_2) \right] \hat{\sigma}_{LO}(s,t,u)(b\bar{b} \to \phi\phi) \tag{1}$$

where $b(x)$ and $\bar{b}(x)$ are the LO parton distribution functions for bottom quarks in the proton, $\hat{\sigma}_{LO}(s,t,u)$ is the parton level cross section for $b\bar{b} \to \phi\phi$ and s,t,u are the Mandelstam variables. Fig. 1 shows the tree level Feynman diagrams for $b\bar{b} \to \phi\phi$ in the MSSM.

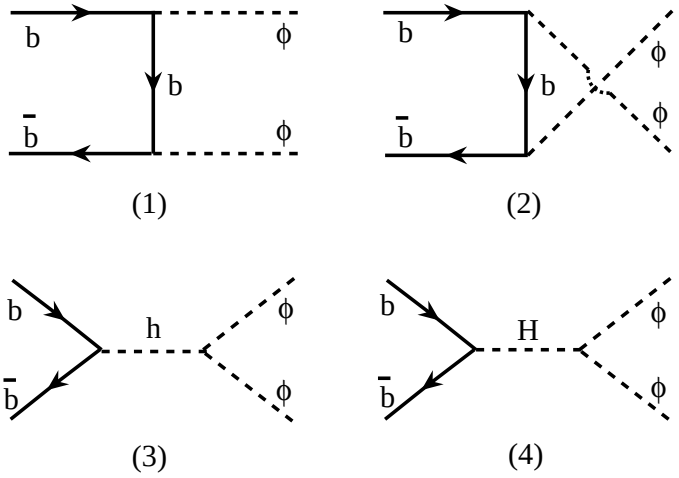


FIG. 1: The lowest order Feynman diagrams in the MSSM for $b\bar{b} \to \phi\phi$, with $\phi = h, H, A$.

We assign momenta to the initial and the final state partons with

$$b(p_1)\bar{b}(p_2) \to \phi(p_3)\phi(p_4)\,, \tag{2}$$

and $p_1 + p_2 = p_3 + p_4$. The $\phi b\bar{b}$ Yukawa coupling, $g_{\phi bb}$, and the $h\phi\phi$ and $H\phi\phi$ trilinear couplings, $g_{h\phi\phi}$ and $g_{H\phi\phi}$, can be found in Appendix C. The lowest order rate can be expressed in terms of spinor structures:

$$\begin{aligned} T_{1L} &= \bar{v}(p_2)P_L u(p_1) \\ T_{1R} &= \bar{v}(p_2)P_R u(p_1)\,, \end{aligned} \tag{3}$$

with $P_{R,L} = (1 \pm \gamma_5)/2$. Following the simplified ACOT prescription [35, 36, 37], we take $m_b = 0$ everywhere except in the Yukawa couplings. The tree level amplitudes of the $s-, t-$

and $u-$ channels are:

$$\begin{aligned}
M_s^0 &= -\left(\frac{g_{hbb}g_{h\phi\phi}}{s-M_h^2+iM_h\Gamma_h}+\frac{g_{Hbb}g_{H\phi\phi}}{s-M_H^2+iM_H\Gamma_H}\right)(T_{1L}+T_{1R})\,\delta_{\alpha\beta}\\
&\equiv \left(X_s^0 T_{1L}+X_s^0 T_{1R}\right)\delta_{\alpha\beta}\\
M_t^0 &= g_{\phi bb}^2\frac{1}{t}(\bar{v}(p_2)\not{p}_3 P_L u(p_1)+\bar{v}(p_2)\not{p}_3 P_R u(p_1))\delta_{\alpha\beta}\\
&\equiv \left(\hat{M}_{tL}^0\delta_{ji}+\hat{M}_{tR}^0\right)\delta_{\alpha\beta}\\
M_u^0 &= -g_{\phi bb}^2\frac{1}{u}(\bar{v}(p_2)\not{p}_3 P_L u(p_1)+\bar{v}(p_2)\not{p}_3 P_R u(p_1))\delta_{\alpha\beta}\\
&\equiv \left(\hat{M}_{uL}^0\delta_{ji}+\hat{M}_{uR}^0\right)\delta_{\alpha\beta}\,,
\end{aligned}\tag{4}$$

where α,β are color indices. The corresponding spin- and color-averaged matrix elements squared, including interferences terms, are

$$\begin{aligned}
\langle|M_t^0|^2\rangle &= \frac{g_{\phi bb}^4}{6}\left(\frac{u}{t}-\frac{M_h^4}{t^2}\right)\\
\langle|M_u^0|^2\rangle &= \frac{g_{\phi bb}^4}{6}\left(\frac{t}{u}-\frac{M_h^4}{u^2}\right)\\
\langle Re(M_t^0\bar{M}_u^0)\rangle &= -\frac{g_{\phi bb}^4}{6}\left(1-\frac{M_h^4}{tu}\right)\\
\langle|M_s^0|^2\rangle &= \frac{g_{hbb}^2 g_{h\phi\phi}^2 s}{6|s-M_h^2+iM_h\Gamma_h|^2}+\frac{g_{Hbb}^2 g_{H\phi\phi}^2 s}{6|s-M_H^2+iM_H\Gamma_H|^2}\\
&\quad+\frac{g_{hbb}g_{Hbb}g_{h\phi\phi}g_{H\phi\phi}}{3}\left(\frac{(s-M_h^2)(s-M_H^2)+M_hM_H\Gamma_h\Gamma_H}{|s-M_h^2+iM_h\Gamma_h|^2\cdot|s-M_H^2+iM_H\Gamma_H|^2}\right)s\,.
\end{aligned}\tag{5}$$

The LO element is then,

$$\begin{aligned}
M_0 &= M_t^0+M_u^0+M_s^0\\
\langle|M_0|^2\rangle &= \langle|M_s^0|^2\rangle+\langle|M_t^0|^2\rangle+\langle|M_u^0|^2\rangle+2\langle Re({M_t}^0\bar{M}_u^0)\rangle\,.
\end{aligned}$$

Finally, the parton level cross section for inclusive $b\bar{b}\to\phi\phi$ production is

$$\hat{\sigma}_{LO} = \int\frac{1}{2s}\frac{1}{2}\langle|M_0|^2\rangle d_2PS(b\bar{b}\to\phi\phi)\,,\tag{6}$$

where $d_2PS(b\bar{b}\to\phi\phi)$ denotes the integral over the two-body phase space and the factor of $1/2$ is from the identical particles in the final state.

III. NEXT-TO-LEADING ORDER CORRECTIONS FOR $b\bar{b}\to\phi\phi$

The parton level NLO cross section is

$$\begin{aligned}
\hat{\sigma}_{\rm NLO}(x_1,x_2,\mu) &= \hat{\sigma}_{\rm LO}(x_1,x_2,\mu)+\delta\hat{\sigma}_{NLO}(x_1,x_2,\mu)\\
&\equiv \hat{\sigma}_{\rm LO}(x_1,x_2,\mu)\left[1+\hat{\delta}_{\rm QCD}(x_1,x_2,\mu)+\hat{\delta}_{\rm SQCD}(x_1,x_2,\mu)\right]\\
\delta\hat{\sigma}_{\rm NLO}(x_1,x_2,\mu) &\equiv \delta\hat{\sigma}_{\rm QCD}(x_1,x_2,\mu)+\delta\hat{\sigma}_{\rm SQCD}(x_1,x_2,\mu)\,,
\end{aligned}\tag{7}$$

where $\hat{\sigma}_{\rm LO}(x_1, x_2, \mu)$ is the leading order (Born) cross section and $\delta\hat{\sigma}_{\rm NLO}(x_1, x_2, \mu)$ is the next-to-leading order correction to the Born cross section, $x_{1,2}$ are the momentum fractions of the partons and $\mu = \mu_R$ is the renormalization scale. The NLO correction $\delta\hat{\sigma}_{NLO}(x_1, x_2, \mu)$ contains both the gluon QCD correction, $\delta\hat{\sigma}_{\rm QCD}(x_1, x_2, \mu)$, and the gluino-squark SQCD correction, $\delta\hat{\sigma}_{\rm SQCD}(x_1, x_2, \mu)$. The gluon QCD correction includes the $O(\alpha_s)$ corrections, which contain virtual and real gluon emission contributions, as well as the $O(1/\Lambda)$ corrections from the $bg \to b\phi\phi$ subprocess. The gluino-squark SQCD correction contains $O(\alpha_s)$ gluino-sbottom loop contributions.

Unlike down-type quarks, which only couple to the down-type Higgs at tree level, the down-type squarks also couple to the up-type Higgs boson. This leads to mixing in the sbottom mass matrix in the $\tilde{b}_L, \tilde{b}_R$ basis,

$$m^2_{\tilde{b}_{1,2}} = \begin{pmatrix} m^2_{\tilde{b}_L} & m_b(A_b - \mu\tan\beta) \\ m_b(A_b - \mu\tan\beta) & m^2_{\tilde{b}_R} \end{pmatrix}, \tag{8}$$

where $\tilde{b}_{1,2}$ are the mass eigenstates. The mass eigenstates $m_{\tilde{b}_1}$ and $m_{\tilde{b}_2}$ ($m_{\tilde{b}_1} \leq m_{\tilde{b}_2}$) are defined in terms of a mixing angle,

$$\begin{pmatrix} \tilde{b}_1 \\ \tilde{b}_2 \end{pmatrix} = \begin{pmatrix} \cos\theta_{\tilde{b}} & \sin\theta_{\tilde{b}} \\ -\sin\theta_{\tilde{b}} & \cos\theta_{\tilde{b}} \end{pmatrix} \begin{pmatrix} \tilde{b}_L \\ \tilde{b}_R \end{pmatrix}. \tag{9}$$

The one-loop virtual gluino-sbottom Feynman diagrams for $b\bar{b} \to \phi\phi$ are shown in Fig. 2. The amplitudes corresponding to each diagram in Fig. 2 are computed analytically and

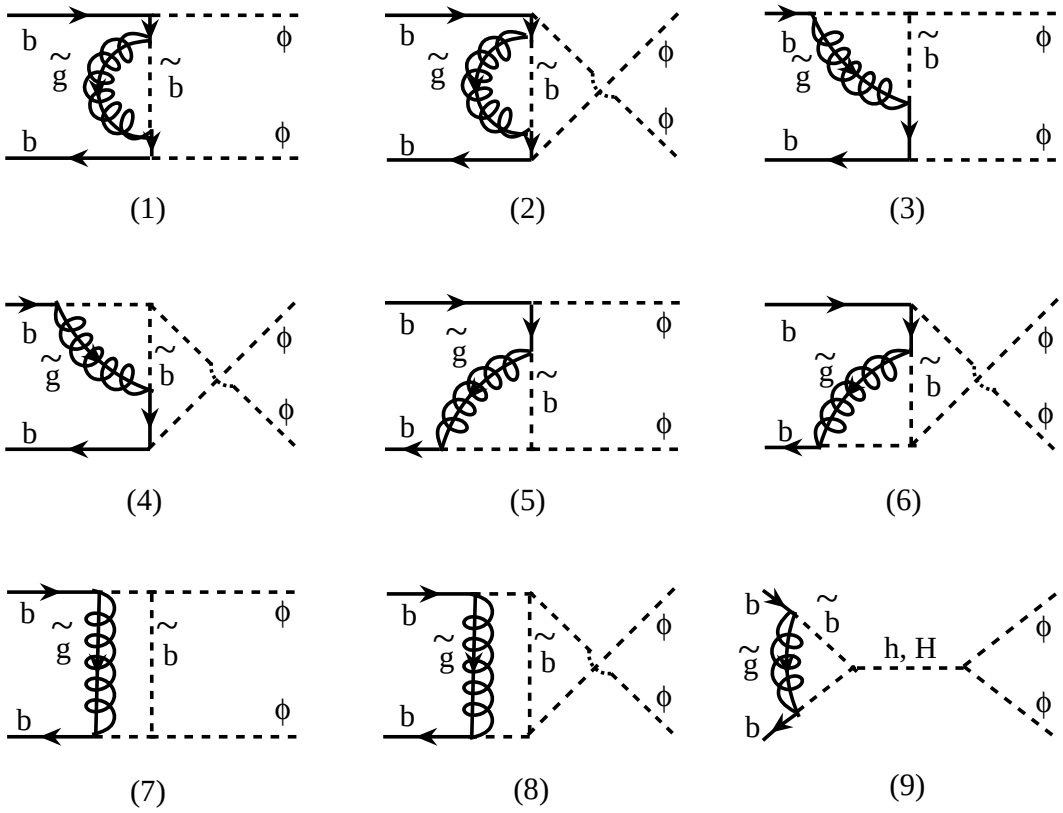


FIG. 2: One-loop SQCD virtual corrections to $b\bar{b} \to \phi\phi$.

all tensor integrals are reduced to linear combinations of one-loop scalar functions. We sum all of the virtual amplitudes to obtain the contribution to the matrix element from gluino-sbottom loops in terms of the standard matrix elements of Eqs. 3 and 4,

$$M_v^{SQCD} = g_s^2(T^aT^a)_{\alpha\beta}\left(\sum_{i=1,3,5,7} X_{i1}\hat{M}^0_{tL} + \sum_{i=1,3,5,7} X_{i2}\hat{M}^0_{tR} + \sum_{i=2,4,6,8} X_{i1}\hat{M}^0_{uL} + \sum_{i=2,4,6,8} X_{i2}\hat{M}^0_{uR} + \sum_{i=1}^{10} X_{i3}T_{1L} + \sum_{i=1}^{10} X_{i4}T_{1R}\right), \quad (10)$$

where i corresponds to the numbering of the diagrams in Fig. 2. The analytic expressions for each coefficient X can be found in appendix B. For simplification, we define:

$$\begin{aligned} X_{tL} &= \sum_{i=1,3,5,7} X_{i1} & X_{tR} &= \sum_{i=1,3,5,7} X_{i2} \\ X_{uL} &= \sum_{i=2,4,6,8} X_{i1} & X_{uR} &= \sum_{i=2,4,6,8} X_{i2} \\ X_L &= \sum_{i=1}^{10} X_{i3} & X_R &= \sum_{i=1}^{10} X_{i4}\,. \end{aligned} \quad (11)$$

The one-loop SQCD matrix element is then

$$M_v^{SQCD} = g_s^2(T^aT^a)_{\alpha\beta}(X_{tR}\hat{M}^0_{tR} + X_{tL}\hat{M}^0_{tL} + X_{uR}\hat{M}^0_{uR} + X_{uL}\hat{M}^0_{uL} + X_L T_{1L} + X_R T_{1R})\,, \quad (12)$$

Only ultraviolet (UV) divergences occur in the SUSY QCD corrections from the massive gluino and squark loops. These UV divergences are removed by the renormalization of the bottom quark wavefunction and propagator and the renormalization of the bottom quark mass in the Yukawa coupling [26, 38, 39, 40, 41, 42]. We use the on-shell renormalization scheme of Ref. [42] and define the b quark self energy as,

$$\begin{aligned} \Sigma^b(p) &= \not{p}\left(\Sigma^b_V(p^2) - \Sigma^b_A(p^2)\gamma_5\right) + m_b\Sigma^b_S(p^2) \\ \delta\Sigma^b(p) &= \not{p}\left(\delta Z^b_V - \delta Z^b_A\gamma_5\right) - m_b\delta Z^b_V - \delta m_b\,, \end{aligned} \quad (13)$$

which gives the renormalized propagator,

$$\Sigma^b_{ren} = (\not{p} - m_b)\left(\Sigma^b_V + \delta Z^b_V\right) + m_b\left(\Sigma^b_V + \Sigma^b_S - \frac{\delta m_b}{m_b}\right). \quad (14)$$

The on-shell renormalization condition requires,

$$\begin{aligned} \Sigma^b(\not{p} = m_b) &= 0 \\ lim_{\not{p}\to m_b}\frac{\Sigma^b(p)}{\not{p} - m_b} &= 0\,. \end{aligned} \quad (15)$$

Computing the bottom quark self energy from gluino-squark loops and ignoring contributions suppressed by powers of m_b, we find:

$$\begin{aligned} \Sigma^b_V(p^2) &= -\frac{\alpha_s}{3\pi}\left[B_1(p, m_{\tilde{g}}, m_{\tilde{b}_1}) + B_1(p, m_{\tilde{g}}, m_{\tilde{b}_2})\right] \\ \Sigma^b_S(p^2) &= -\frac{\alpha_s}{3\pi}\left(\frac{m_{\tilde{g}}}{m_b}\right)\sin 2\theta_{\tilde{b}}\left[B_0(p, m_{\tilde{g}}, m_{\tilde{b}_2}) - B_0(p, m_{\tilde{g}}, m_{\tilde{b}_1})\right], \end{aligned} \quad (16)$$

which yields,

$$\begin{aligned}\delta Z_V^b &= -\Sigma_V^b|_{p^2=m_b^2} \\ \frac{\delta m_b}{m_b} &= (\Sigma_V + \Sigma_S)\,|_{p^2=m_b^2}\,. \end{aligned} \tag{17}$$

The coupling of the b squark to the up-type Higgs doublet induces a modification of the tree-level relation between the bottom quark mass and its Yukawa coupling. At large $\tan\beta$, we absorb this modification by redefining the bottom quark mass occuring in the Yukawa coupling,[19, 43, 44, 45, 46]

$$m_b \to \frac{m_b}{1+\Delta_b}\,, \tag{18}$$

where

$$\Delta_b = \frac{2\alpha_s(\mu_R)}{3\pi} m_{\tilde{g}}\mu\tan\beta I(m_{\tilde{b}_1}, m_{\tilde{b}_2}, m_{\tilde{g}}) \quad . \tag{19}$$

and the auxiliary function is defined as,

$$I(a,b,c) = -\frac{1}{(a^2-b^2)(b^2-c^2)(c^2-a^2)}(a^2b^2\ln\frac{a^2}{b^2} + b^2c^2\ln\frac{b^2}{c^2} + c^2a^2\ln\frac{c^2}{a^2}) \quad . \tag{20}$$

The contributions to the bottom Yukawa couplings which are enhanced at large $\tan\beta$ can be included to all orders by making the following replacements [19, 43, 44, 45, 46]:

$$\begin{aligned} g_{hbb} &\to g_{hbb}\frac{1-\Delta_b/(\tan\beta\tan\alpha)}{1+\Delta_b} \\ g_{Hbb} &\to g_{Hbb}\frac{1+\Delta_b\tan\alpha/\tan\beta}{1+\Delta_b} \\ g_{Abb} &\to g_{Abb}\frac{1-\Delta_b/\tan^2\beta}{1+\Delta_b}\,. \end{aligned}$$

We use these effective Yukawa couplings in our NLO computation. To avoid double-counting, we add additional mass counterterms,

$$\frac{\delta\tilde{m}_b^h}{m_b} = \Delta_b\left(1+\frac{1}{\tan\alpha\tan\beta}\right), \quad \frac{\delta\tilde{m}_b^H}{m_b} = \Delta_b\left(1-\frac{\tan\alpha}{\tan\beta}\right), \quad \frac{\delta\tilde{m}_b^A}{m_b} = \Delta_b\left(1+\frac{1}{\tan^2\beta}\right), \tag{21}$$

for h, H and A production, respectively.

The counterterms arise from the b quark wavefunction renormalization (a factor of $\delta Z_b/2$ for each external b quark), the b mass renormalization in the $\phi b\overline{b}$ couplings (this occurs twice in the $t-$ and $u-$ channel diagrams, and once in the $s-$channel diagram), and a factor of $-\delta Z_V$ from the mass renormalization on the internal b quark propagators shown in Fig. 3:

$$M_{CT} = 2\Big(\frac{\delta m_b}{m_b} + \frac{\delta\tilde{m}_b^\phi}{m_b}\Big)(M_t^0 + M_u^0) + \Big(\delta Z_V + \frac{\delta m_b}{m_b} + \frac{\delta\tilde{m}_b^\phi}{m_b}\Big)M_s^0\,. \tag{22}$$

The complete one-loop SUSY QCD contribution is,

$$M^{SQCD} = M_0 + M_v^{SQCD} + M_{CT}\,, \tag{23}$$

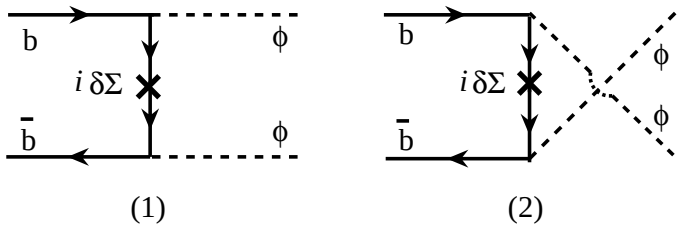


FIG. 3: $t-$ and $u-$ channel bottom quark propagator counterterm diagrams.

and is of course finite. Finally, the SQCD contribution to the matrix element squared is,

$$\begin{aligned} |M^{SQCD}|^2 &\equiv \mid M_0 \mid^2 + 2Re(M_v^{SQCD}\overline{M_0}) + 2Re(M_{CT}\overline{M_0}) \\ &= \mid M_0 \mid^2 + 2Re(M_v^{SQCD}\overline{M_0}) + 4(\frac{\delta m_b}{m_b} + \frac{\delta\tilde{m}_b^{\phi}}{m_b})|M_t^0 + M_u^0|^2 \\ &\quad + 2(\delta Z_V + \frac{\delta m_b}{m_b} + \frac{\delta\tilde{m}_b^{\phi}}{m_b})|M_s^0|^2 \end{aligned} \tag{24}$$

with the spin and color averaged result,

$$\begin{aligned} 2\langle Re(M_v^{SQCD}\overline{M_0})\rangle &= \frac{4\pi\alpha_s}{9}\Big\{(X_{tR}+X_{tL})|M_t^0|^2 + (X_{uR}+X_{uL})|M_u^0|^2 \\ &+ (X_{tR}+X_{uR}+X_{tL}+X_{uL})Re(M_t^0\overline{M}_u^0) \\ &+ 2Re[(X_L+X_R)X_s^{0*}]s\Big\} \ . \end{aligned} \tag{25}$$

IV. RESULTS FOR HIGGS PAIR PRODUCTION FROM BOTTOM QUARK FUSION

In this section, we present the next-to-leading-order inclusive cross sections for the production of a pair of neutral Higgs bosons via bottom quark fusion in the MSSM and mSUGRA models at the CERN LHC. As in our previous paper [10], we use the lowest order CTEQ6L1 parton distribution functions (PDFs) [47] with a factorization scale μ_F and the leading-order evolution of the strong coupling $\alpha_s(\mu_R)$ with a renormalization scale μ_R to calculate the LO cross sections and use the CTEQ6M PDFs with the next-to-leading-order evolution of $\alpha_s(\mu_R)$ to evaluate the NLO inclusive cross sections. For simplification, we use the same renormalization and factorization scales $\mu_F = \mu_R$. We evaluate the bottom quark mass occuring in the $\phi b\overline{b}$ Yukawa couplings using the $\overline{MS}$ mass, $\overline{m}_b(\mu)$, with a two-loop heavy quark running mass with $m_b(pole) = 4.7\ GeV$ and the NLO evolution of the strong coupling constant, modified to decouple the effects of the top quark[48, 49, 50]. The Higgs couplings are in Appendix C [2, 51, 52, 53] and we compute the Higgs boson masses to one-loop accuracy [54].

A. Results in the Minimal Supersymmetric Model (MSSM)

In Fig. 4, we show the LO and NLO cross sections versus the pseudoscalar Higgs mass M_A. We assume $m_{\tilde{g}} = m_{\tilde{b_L}} = m_{\tilde{b_R}} = -A_b = \mu = M_{SUSY}$ and compute the b squark masses

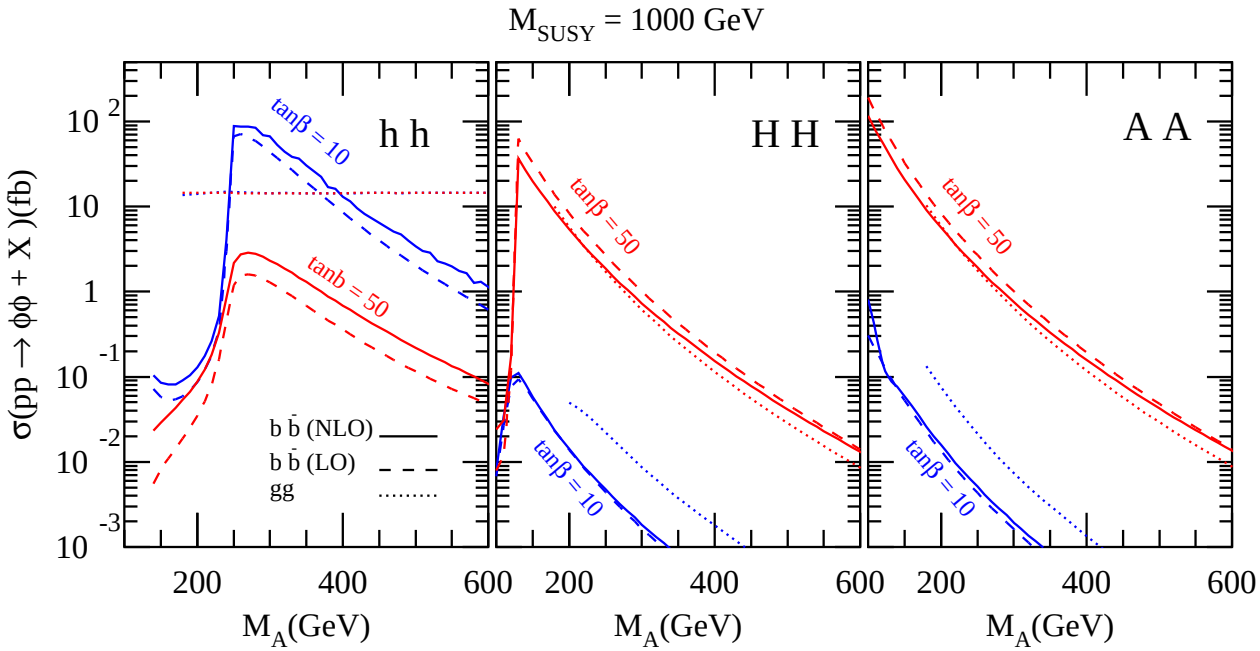


FIG. 4: Next-to-leading order cross sections $\sigma_{NLO}(pp \to \phi\phi + X)$ (solid) and leading order cross sections $\sigma_{LO}(pp \to \phi\phi + X)$ (dash) for Higgs pair production from bottom quark fusion versus the pseudoscalar Higgs mass (M_A) with $\sqrt{S} = 14$ TeV and $\mu_R = \mu_F = M_\phi/2$. The NLO cross sections include both the pure QCD and the SQCD corrections. We use $\tan\beta = 50$ (red) and $\tan\beta = 10$ (blue) with $M_{SUSY} = 1000$ GeV. Also shown are the cross sections of gg fusion (dot).

and mixing angles from Eqa. 8 and 9. Our NLO cross sections include the $\mathcal{O}(\alpha_s)$ corrections from the $b\overline{b}$ initial state and the $\mathcal{O}(1/\Lambda)$ corrections from the bg initial state, along with the SQCD corrections from gluino-sbottom loops. We show our results with $\tan\beta = 50$ (red) and $\tan\beta = 10$ (blue) at $M_{SUSY} = 1000$ GeV. To compare with gg fusion, we also plot the cross section from the gg initial state (dot) [5, 8]. We note that the cross sections for Higgs pair production in the MSSM are significantly larger than in the standard model, due to enhancements at large $\tan\beta$. The resonant enhancements due to $s-$ channel scalar exchange are clearly visible in the $b\overline{b} \to hh$ and $b\overline{b} \to HH$ curves. At $\tan\beta = 10$, the cross section for pair of the lightest neutral Higgs boson (hh) from $b\overline{b}$ fusion is much larger than the cross section from the gluon-gluon initial state, while the rate for pair production of the heavier neutral Higgs bosons (HH and AA) from $b\overline{b}$ fusion is highly suppressed relative to the gluon-gluon production. But at $\tan\beta = 50$, gluon fusion dominates pair of the lightest neutral Higgs boson (hh) production and is comparible with $b\overline{b}$ production for the heavier neutral Higgs bosons (HH and AA) production.

Figs. 5 and Fig. 6 show the NLO cross sections versus M_A with $M_{SUSY} = 1000$ GeV and $\tan\beta = 50$. We present the NLO cross section with only gluon QCD corrections (dash-dot-dot,green), NLO cross section with only gluino-sbottom SQCD corrections (dot,blue),and the complete NLO cross section with QCD and SQCD corrections together (dash, red). We note:

- The NLO SQCD correction to $b\bar{b} \to hh$ is small. The dominant contribution to the NLO correction to light Higgs pair production is from the pure QCD contribution.
- For heavy Higgs pair and pseudoscalar Higgs pair production, the SUSY QCD cor-

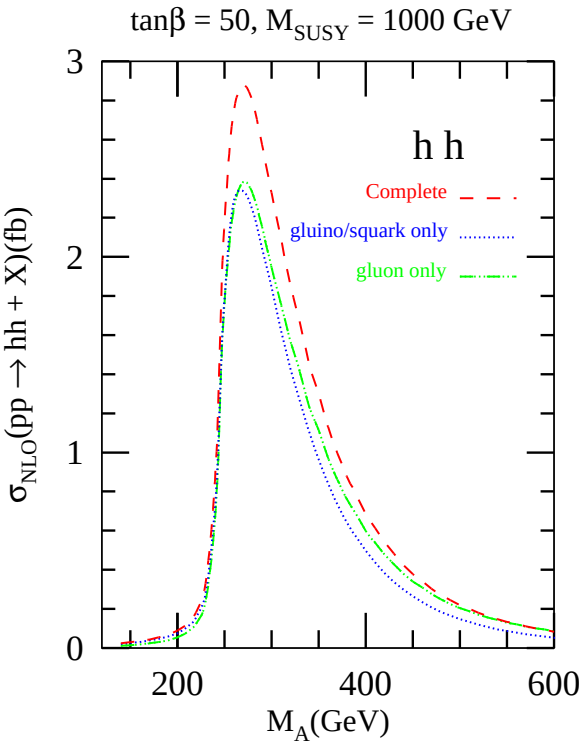


FIG. 5: Next-to-leading order cross section $\sigma_{NLO}(pp \to hh+X)$ in bottom quark fusion versus M_A with $\sqrt{S} = 14$ TeV, $\tan\beta = 50$ and $M_{SUSY} = 1000$ GeV. We plot the NLO cross section with only gluon QCD correction (dash-dot-dot, green), NLO cross section with only gluino-sbottom SQCD correction (dot, blue) and complete NLO cross section with both gluon QCD and gluino-sbottom SQCD corrections (dash, red).

rections become dominant. The pure gluon NLO contribution is much smaller in magnitude than the contribution from SQCD.

In Fig. 7, we plot the ratio of the NLO SQCD correction normalized to the Born cross section, $\delta_{\rm SQCD}$, with $M_A = m_{\tilde{g}} = -A_b = 1000$ GeV, and $\tan\beta = 10$ (dash-dot-dot, green), $tan\beta = 30$ (dash, blue) and $tan\beta = 50$ (solid, red). In the limit of large squark masses, δ_{SQCD} approaches a common non-zero constant for HH and AA production. Light Higgs pair production, however, decouples for large M_A and large SUSY masses. This decoupling behaviour is also seen in the decay $h \to b\overline{b}$ [45, 55] and the production process $bg \to bh$[26].

In Fig. 8, we fix M_A and all squark masses to be 1000 GeV and plot δ_{SQCD} versus the gluino mass $m_{\tilde{g}}$ with $tan\beta = 10$ (dash-dot-dot, green), $tan\beta = 30$ (dash, blue) and $tan\beta = 50$ (solid, red). This figure does not demonstrate a decoupling behaviour.

B. Results in the Minimal Supergravity Model (mSUGRA)

In this model, supersymmetry is assumed to be broken in a hidden sector consisting of fields that interact with the usual particles and their superpartners only via gravity. Supersymmetry breaking is communicated to the visible sector via gravitational interactions. Within the mSUGRA framework, it is assumed that at some high scale (frequently taken to be $\sim M_{GUT}$) all scalar fields have a common SUSY breaking mass M_0, all gauginos have a

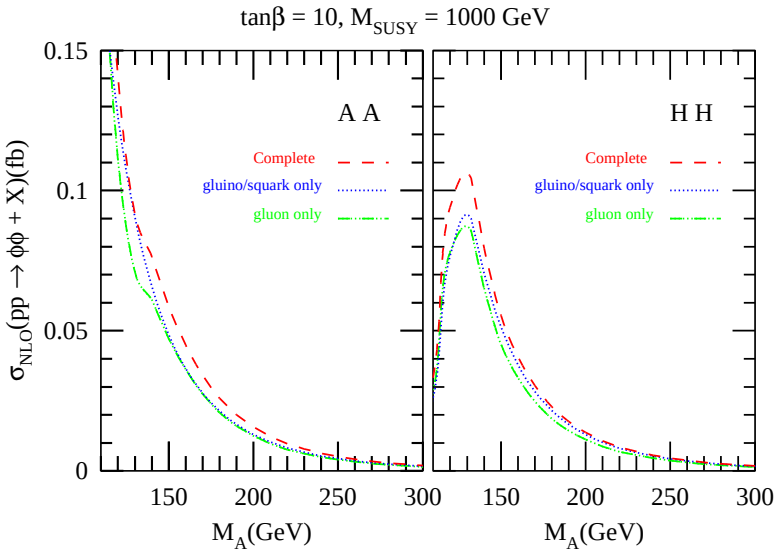


FIG. 6: Next-to-leading order cross sections for (a) $\sigma_{NLO}(pp \to HH+X)$ and (b) $\sigma_{NLO}(pp \to AA+X)$ from bottom quark fusion versus M_A with $\sqrt{S} = 14$ TeV, $\tan\beta = 50$ and $M_{SUSY} = 1000$ GeV. We plot the NLO cross section with only gluon QCD correction (dash-dot-dot, green), NLO cross section with only gluino-sbottom SQCD correction (dot, blue) and complete NLO cross section with both gluon QCD and gluino-sbottom SQCD corrections (dash, red).

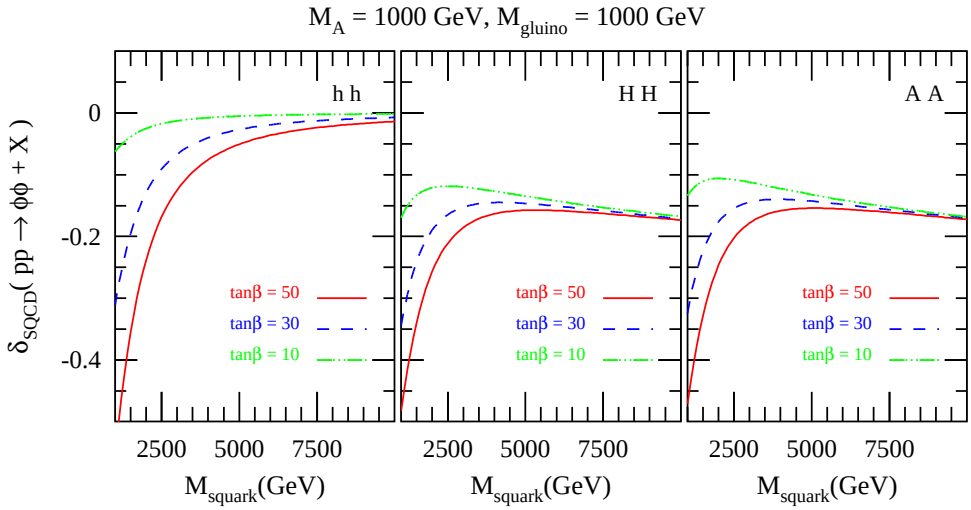


FIG. 7: δ_{SQCD} versus squark mass $m_{\tilde{q}}$ with $M_A = m_{\tilde{g}} = 1000$ GeV and $\sqrt{S} = 14$ TeV for (a) $b\bar{b} \to hh$, (b) $b\bar{b} \to HH$ and (c) $b\bar{b} \to AA$. $\tan\beta = 10$ (dash-dot-dot, green),$\tan\beta = 30$ (dash, blue) and $\tan\beta = 50$ (solid, red).

common mass $M_{1/2}$, and all soft SUSY breaking scalar trilinear couplings have a common value A_0. Electroweak symmetry breaking is assumed to occur radiatively. This fixes the magnitude of the superpotential parameter μ. The soft SUSY breaking bilinear Higgs boson mass parameter can be eliminated in favour of $\tan\beta$, so that the model is completely specified by the parameter set:

$$M_0,\ M_{1/2},\ A_0,\ \tan\beta,\ sign(\mu). \tag{26}$$

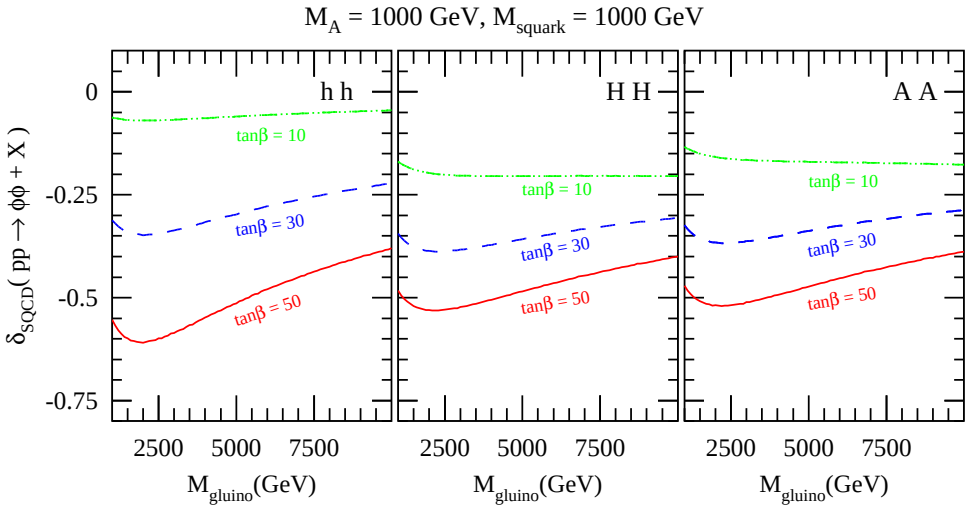


FIG. 8: δ_{SQCD} versus gluino mass, $m_{\tilde{g}}$, with $M_A = m_{\tilde{b_{L,R}}} = \mu = 1000$ GeV and $\sqrt{S} = 14$ TeV for (a) $b\bar{b} \to hh$, (b) $b\bar{b} \to HH$ and (c) $b\bar{b} \to AA$. $\tan\beta = 10$ (dash-dot-dot, green),$\tan\beta = 30$ (dash, blue) and $\tan\beta = 50$ (solid, red).

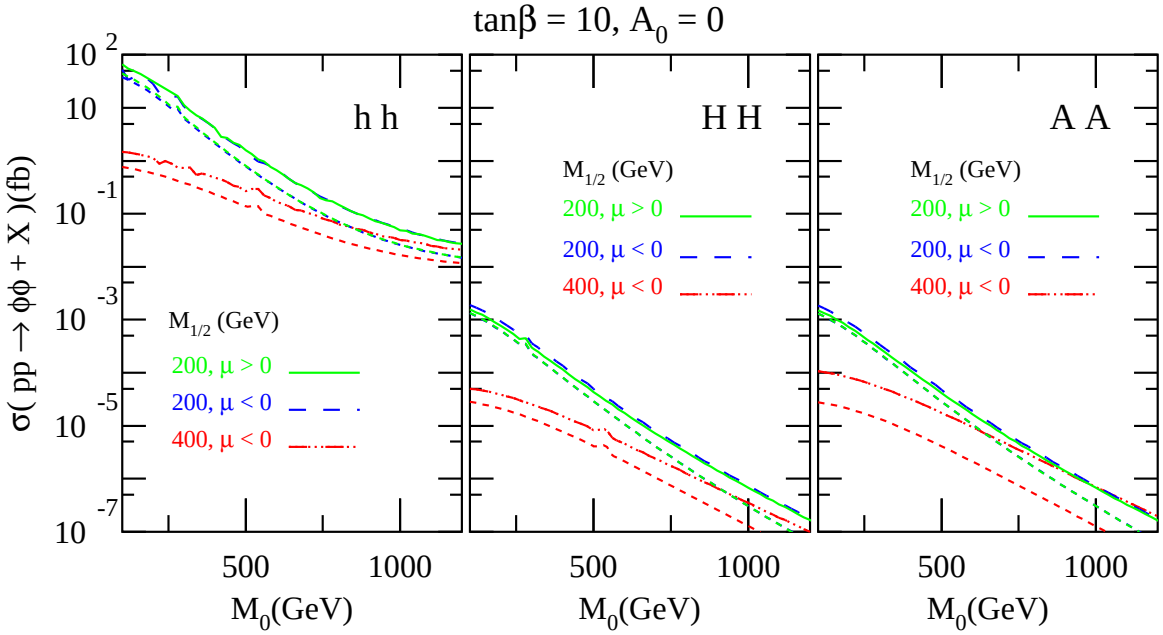


FIG. 9: σ_{NLO} versus M_0 with $\sqrt{S} = 14$ TeV and $\tan\beta = 10$. Three cases are shown with $\mu > 0$ for $M_{1/2} = 200$ (blue)and 400 GeV (red), $\mu < 0$ for $M_{1/2} = 200$ GeV(green). Also shown are the LO cross sections, $\sigma_{\rm LO}$ (dot).

All the sparticle masses and couplings required for phenomenological analysis can be obtained via renormalization group evolution between the scale of grand unification and the weak scale.

We show the LO (dot) and NLO (solid) cross sections versus M_0 with $A_0 = 0$ for $\tan\beta = 10$ in Fig. 9 and $\tan\beta = 50$ in Fig. 10. We plot six curves in each frame, three LO cross sections (dot) and three NLO cross sections (solid). The NLO curves include both the pure

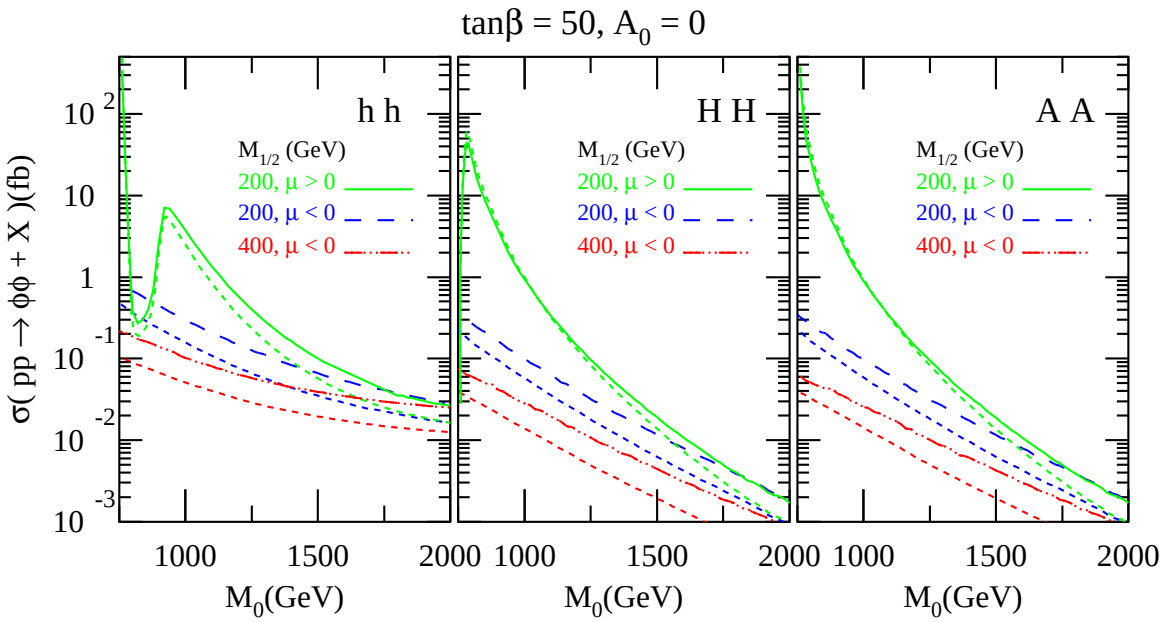


FIG. 10: σ_{NLO} versus M_0 with $\sqrt{S} = 14$ TeV and $\tan\beta = 50$. Three cases are shown with $\mu > 0$ for $M_{1/2} = 200$ (blue) and 400 GeV (red), $\mu < 0$ for $M_{1/2} = 200$ GeV(green). Also shown are the LO cross sections, $\sigma_{\rm LO}$ (dot).

QCD and the SQCD contributions. As shown in the graphs, blue lines are cross sections with $M_{1/2} = 200$ GeV, $\mu < 0$, green lines have $M_{1/2} = 200$ GeV, $\mu > 0$, and red lines are for $M_{1/2} = 400$ GeV, $\mu < 0$. Comparing Figs. 9 and 10 we see a strong dependence on $\tan\beta$.

- When $\tan\beta = 10$, flipping the sign of μ has little effect on either the LO or the NLO cross sections with $M_{1/2} = 200$ GeV. As $\tan\beta$ increases to 50, we notice that flipping the sign of μ has a large effect when $M_0 < 1200$ GeV as shown in Fig. 10.

- For large M_0, the cross sections approach a common value, independent of $M_{1/2}$ and μ.

V. CONCLUSIONS

In this paper we presented the complete $\mathcal{O}(\alpha_s)$ SUSY QCD corrections to neutral Higgs pair production from bottom quark fusion in the Minimal Supersymmetric Model and the Minimal Supergravity Model at the CERN LHC. The effects of the SUSY QCD corrections from sbottom and gluino loops are significant in some regions of parameter space and the decoupling of the SQCD effects is only recovered for light Higgs pair production in the large M_A limit.

Acknowledgments

We are grateful to Jianwei Qiu and Chris Jackson for beneficial discussions. This research was supported in part by the U.S. Department of Energy under Grants No. DE-AC02-76CH1-

886, No. DE-FG02-04ER41305, No. DE-FG02-03ER46040 and DE-AC02-98CH10886. SD thanks the SLAC theory group for their hospitality, where this work was completed.

APPENDIX A: THE SCALAR INTEGRALS

$$\begin{aligned}
\frac{i}{16\pi^2}B_0(p,m_1,m_2) &= \int\frac{d^nk}{(2\pi)^n}\frac{1}{(k^2-m_1^2)[(k+p)^2-m_2^2]}\\
\frac{i}{16\pi^2}\not{p}B_{11}(p,m_1,m_2) &= \int\frac{d^nk}{(2\pi)^n}\frac{\not{k}}{(k^2-m_1^2)[(k+p)^2-m_2^2]}\\
\frac{i}{16\pi^2}C_0(p_1,p_2,m_1,m_2,m_3) &= \int\frac{d^nk}{(2\pi)^n}\frac{1}{(k^2-m_1^2)[(k+p_1)^2-m_2^2][(k+p_1+p_2)^2-m_3^2]}
\end{aligned}$$

$$\begin{aligned}
&\frac{i}{16\pi^2}\Big(\not{p}_1C_{11}(p_1,p_2,m_1,m_2,m_3)+\not{p}_2C_{12}(p_1,p_2,m_1,m_2,m_3)\Big)\\
&=\int\frac{d^nk}{(2\pi)^n}\frac{\not{k}}{(k^2-m_1^2)[(k+p_1)^2-m_2^2][(k+p_1+p_2)^2-m_3^2]}
\end{aligned}$$

$$\begin{aligned}
&\frac{i}{16\pi^2}\Big(\not{p}_1D_{11}(p_1,p_2,p_3,m_1,m_2,m_3,m_4)+\not{p}_2D_{12}(p_1,p_2,p_3,m_1,m_2,m_3,m_4)\\
&+\not{p}_3D_{13}(p_1,p_2,m_1,m_2,m_3,m_4)\Big)\\
&=\int\frac{d^nk}{(2\pi)^n}\frac{\not{k}}{(k^2-m_1^2)[(k+p_1)^2-m_2^2][(k+p_1+p_2)^2-m_3^2][(k+p_1+p_2+p_3)^2-m_4^2]}
\end{aligned}$$

$$\begin{aligned}
&D_{123}(p_1,p_2,p_3,m_1,m_2,m_3,m_4)\\
&=D_{12}(p_1,p_2,p_3,m_1,m_2,m_3,m_4)-D_{13}(p_1,p_2,p_3,m_1,m_2,m_3,m_4)
\end{aligned}$$

APPENDIX B: X COEFFICIENTS

1. X coefficients for $b\bar{b}\to hh$ and $b\bar{b}\to HH$

$$\begin{aligned}
X_{11} &= \frac{1}{8\pi^2}\Big[B_1(-p_1+p_3,m_{\tilde{g}},m_{\tilde{b}_1})\sin^2\theta_{\tilde{b}}+B_1(-p_1+p_3,m_{\tilde{g}},m_{\tilde{b}_2})\cos^2\theta_{\tilde{b}}\Big]\\
X_{12} &= \frac{1}{8\pi^2}\Big[B_1(-p_1+p_3,m_{\tilde{g}},m_{\tilde{b}_1})\cos^2\theta_{\tilde{b}}+B_1(-p_1+p_3,m_{\tilde{g}},m_{\tilde{b}_2})\sin^2\theta_{\tilde{b}}\Big]\\
X_{13} &= -\frac{1}{8\pi^2}\frac{g^2_{\phi bb}}{t}m_{\tilde{g}}\Big[B_0(-p_1+p_3,m_{\tilde{g}},m_{\tilde{b}_1})-B_0(-p_1+p_3,m_{\tilde{g}},m_{\tilde{b}_2})\Big]\sin\theta_{\tilde{b}}\cos\theta_{\tilde{b}}\\
X_{14} &= X_{13}
\end{aligned}$$

$$X_{2i} = X_{1i}(t\leftrightarrow u, p_3\leftrightarrow p_4)\quad i=1,2,3,4$$

$$
\begin{aligned}
X_{31} &= \frac{1}{8\pi^2}\frac{g_{\phi 11}}{g_{\phi bb}} m_{\tilde{g}} C_0(-p_1,p_3,m_{\tilde{g}},m_{\tilde{b}_1},m_{\tilde{b}_1})\sin\theta_{\tilde{b}}\cos\theta_{\tilde{b}} \\
&+ \frac{1}{8\pi^2}\frac{g_{\phi 12}}{g_{\phi bb}} m_{\tilde{g}} C_0(-p_1,p_3,m_{\tilde{g}},m_{\tilde{b}_1},m_{\tilde{b}_2})\cos^2\theta_{\tilde{b}} \\
&- \frac{1}{8\pi^2}\frac{g_{\phi 12}}{g_{\phi bb}} m_{\tilde{g}} C_0(-p_1,p_3,m_{\tilde{g}},m_{\tilde{b}_2},m_{\tilde{b}_1})\sin^2\theta_{\tilde{b}} \\
&- \frac{1}{8\pi^2}\frac{g_{\phi 22}}{g_{\phi bb}} m_{\tilde{g}} C_0(-p_1,p_3,m_{\tilde{g}},m_{\tilde{b}_2},m_{\tilde{b}_2})\sin\theta_{\tilde{b}}\cos\theta_{\tilde{b}} \\
X_{32} &= \frac{1}{8\pi^2}\frac{g_{\phi 11}}{g_{\phi bb}} m_{\tilde{g}} C_0(-p_1,p_3,m_{\tilde{g}},m_{\tilde{b}_1},m_{\tilde{b}_1})\sin\theta_{\tilde{b}}\cos\theta_{\tilde{b}} \\
&- \frac{1}{8\pi^2}\frac{g_{\phi 12}}{g_{\phi bb}} m_{\tilde{g}} C_0(-p_1,p_3,m_{\tilde{g}},m_{\tilde{b}_1},m_{\tilde{b}_2})\sin^2\theta_{\tilde{b}} \\
&+ \frac{1}{8\pi^2}\frac{g_{\phi 12}}{g_{\phi bb}} m_{\tilde{g}} C_0(-p_1,p_3,m_{\tilde{g}},m_{\tilde{b}_2},m_{\tilde{b}_1})\cos^2\theta_{\tilde{b}} \\
&- \frac{1}{8\pi^2}\frac{g_{\phi 22}}{g_{\phi bb}} m_{\tilde{g}} C_0(-p_1,p_3,m_{\tilde{g}},m_{\tilde{b}_2},m_{\tilde{b}_2})\sin\theta_{\tilde{b}}\cos\theta_{\tilde{b}} \\
X_{33} &= -\frac{1}{8\pi^2} g_{\phi bb} g_{\phi 11} C_{12}(-p_1,p_3,m_{\tilde{g}},m_{\tilde{b}_1},m_{\tilde{b}_1})\cos^2\theta_{\tilde{b}} \\
&+ \frac{1}{8\pi^2} g_{\phi bb} g_{\phi 12} C_{12}(-p_1,p_3,m_{\tilde{g}},m_{\tilde{b}_1},m_{\tilde{b}_2})\sin\theta_{\tilde{b}}\cos\theta_{\tilde{b}} \\
&+ \frac{1}{8\pi^2} g_{\phi bb} g_{\phi 12} C_{12}(-p_1,p_3,m_{\tilde{g}},m_{\tilde{b}_2},m_{\tilde{b}_1})\sin\theta_{\tilde{b}}\cos\theta_{\tilde{b}} \\
&- \frac{1}{8\pi^2} g_{\phi bb} g_{\phi 22} C_{12}(-p_1,p_3,m_{\tilde{g}},m_{\tilde{b}_2},m_{\tilde{b}_2})\sin^2\theta_{\tilde{b}} \\
X_{34} &= -\frac{1}{8\pi^2} g_{\phi bb} g_{\phi 11} C_{12}(-p_1,p_3,m_{\tilde{g}},m_{\tilde{b}_1},m_{\tilde{b}_1})\sin^2\theta_{\tilde{b}} \\
&- \frac{1}{8\pi^2} g_{\phi bb} g_{\phi 12} C_{12}(-p_1,p_3,m_{\tilde{g}},m_{\tilde{b}_1},m_{\tilde{b}_2})\sin\theta_{\tilde{b}}\cos\theta_{\tilde{b}} \\
&- \frac{1}{8\pi^2} g_{\phi bb} g_{\phi 12} C_{12}(-p_1,p_3,m_{\tilde{g}},m_{\tilde{b}_2},m_{\tilde{b}_1})\sin\theta_{\tilde{b}}\cos\theta_{\tilde{b}} \\
&- \frac{1}{8\pi^2} g_{\phi bb} g_{\phi 22} C_{12}(-p_1,p_3,m_{\tilde{g}},m_{\tilde{b}_2},m_{\tilde{b}_2})\cos^2\theta_{\tilde{b}}
\end{aligned}
$$

$$
X_{4i} = X_{3i}(t \leftrightarrow u, p_3 \leftrightarrow p_4) \quad i = 1,2,3,4
$$

$$
\begin{aligned}
X_{51} &= \frac{1}{8\pi^2}\frac{g_{\phi 11}}{g_{\phi bb}} m_{\tilde{g}} C_0(p_2,-p_4,m_{\tilde{g}},m_{\tilde{b}_1},m_{\tilde{b}_1})\sin\theta_{\tilde{b}}\cos\theta_{\tilde{b}} \\
&- \frac{1}{8\pi^2}\frac{g_{\phi 12}}{g_{\phi bb}} m_{\tilde{g}} C_0(p_2,-p_4,m_{\tilde{g}},m_{\tilde{b}_2},m_{\tilde{b}_1})\sin^2\theta_{\tilde{b}} \\
&+ \frac{1}{8\pi^2}\frac{g_{\phi 12}}{g_{\phi bb}} m_{\tilde{g}} C_0(p_2,-p_4,m_{\tilde{g}},m_{\tilde{b}_1},m_{\tilde{b}_2})\cos^2\theta_{\tilde{b}} \\
&- \frac{1}{8\pi^2}\frac{g_{\phi 22}}{g_{\phi bb}} m_{\tilde{g}} C_0(p_2,-p_4,m_{\tilde{g}},m_{\tilde{b}_2},m_{\tilde{b}_2})\sin\theta_{\tilde{b}}\cos\theta_{\tilde{b}}
\end{aligned}
$$

$$
\begin{aligned}
X_{52} &= \frac{1}{8\pi^2}\frac{g_{\phi 11}}{g_{\phi bb}} m_{\tilde{g}} C_0(p_2,-p_4,m_{\tilde{g}},m_{\tilde{b}_1},m_{\tilde{b}_1})\sin\theta_{\tilde{b}}\cos\theta_{\tilde{b}} \\
&+ \frac{1}{8\pi^2}\frac{g_{\phi 12}}{g_{\phi bb}} m_{\tilde{g}} C_0(p_2,-p_4,m_{\tilde{g}},m_{\tilde{b}_2},m_{\tilde{b}_1})\cos^2\theta_{\tilde{b}} \\
&- \frac{1}{8\pi^2}\frac{g_{\phi 12}}{g_{\phi bb}} m_{\tilde{g}} C_0(p_2,-p_4,m_{\tilde{g}},m_{\tilde{b}_1},m_{\tilde{b}_2})\sin^2\theta_{\tilde{b}} \\
&- \frac{1}{8\pi^2}\frac{g_{\phi 22}}{g_{\phi bb}} m_{\tilde{g}} C_0(p_2,-p_4,m_{\tilde{g}},m_{\tilde{b}_2},m_{\tilde{b}_2})\sin\theta_{\tilde{b}}\cos\theta_{\tilde{b}} \\
X_{53} &= -\frac{1}{8\pi^2} g_{\phi bb} g_{\phi 11} C_{12}(p_2,-p_4,m_{\tilde{g}},m_{\tilde{b}_1},m_{\tilde{b}_1})\sin^2\theta_{\tilde{b}} \\
&- \frac{1}{8\pi^2} g_{\phi bb} g_{\phi 12} C_{12}(p_2,-p_4,m_{\tilde{g}},m_{\tilde{b}_2},m_{\tilde{b}_1})\sin\theta_{\tilde{b}}\cos\theta_{\tilde{b}} \\
&- \frac{1}{8\pi^2} g_{\phi bb} g_{\phi 12} C_{12}(p_2,-p_4,m_{\tilde{g}},m_{\tilde{b}_1},m_{\tilde{b}_2})\sin\theta_{\tilde{b}}\cos\theta_{\tilde{b}} \\
&- \frac{1}{8\pi^2} g_{\phi bb} g_{\phi 22} C_{12}(p_2,-p_4,m_{\tilde{g}},m_{\tilde{b}_2},m_{\tilde{b}_2})\cos^2\theta_{\tilde{b}} \\
X_{54} &= -\frac{1}{8\pi^2} g_{\phi bb} g_{\phi 11} C_{12}(p_2,-p_4,m_{\tilde{g}},m_{\tilde{b}_1},m_{\tilde{b}_1})\cos^2\theta_{\tilde{b}} \\
&+ \frac{1}{8\pi^2} g_{\phi bb} g_{\phi 12} C_{12}(p_2,-p_4,m_{\tilde{g}},m_{\tilde{b}_2},m_{\tilde{b}_1})\sin\theta_{\tilde{b}}\cos\theta_{\tilde{b}} \\
&+ \frac{1}{8\pi^2} g_{\phi bb} g_{\phi 12} C_{12}(p_2,-p_4,m_{\tilde{g}},m_{\tilde{b}_1},m_{\tilde{b}_2})\sin\theta_{\tilde{b}}\cos\theta_{\tilde{b}} \\
&- \frac{1}{8\pi^2} g_{\phi bb} g_{\phi 22} C_{12}(p_2,-p_4,m_{\tilde{g}},m_{\tilde{b}_2},m_{\tilde{b}_2})\sin^2\theta_{\tilde{b}}
\end{aligned}
$$

$$
X_{6i} = X_{5i}(t \leftrightarrow u, p_3 \leftrightarrow p_4) \quad i = 1,2,3,4
$$

$$
\begin{aligned}
X_{71} &= \frac{1}{8\pi^2}\frac{g_{\phi 11}^2}{g_{\phi bb}^2} tD_{123}(-p_1,p_3,p_4,m_{\tilde{g}},m_{\tilde{b}_1},m_{\tilde{b}_1},m_{\tilde{b}_1})\cos^2\theta_{\tilde{b}} \\
&- \frac{1}{8\pi^2}\frac{g_{\phi 11} g_{\phi 12}}{g_{\phi bb}^2} tD_{123}(-p_1,p_3,p_4,m_{\tilde{g}},m_{\tilde{b}_1},m_{\tilde{b}_1},m_{\tilde{b}_2})\sin\theta_{\tilde{b}}\cos\theta_{\tilde{b}} \\
&+ \frac{1}{8\pi^2}\frac{g_{\phi 12}^2}{g_{\phi bb}^2} tD_{123}(-p_1,p_3,p_4,m_{\tilde{g}},m_{\tilde{b}_1},m_{\tilde{b}_2},m_{\tilde{b}_1})\cos^2\theta_{\tilde{b}} \\
&- \frac{1}{8\pi^2}\frac{g_{\phi 22} g_{\phi 12}}{g_{\phi bb}^2} tD_{123}(-p_1,p_3,p_4,m_{\tilde{g}},m_{\tilde{b}_1},m_{\tilde{b}_2},m_{\tilde{b}_2})\sin\theta_{\tilde{b}}\cos\theta_{\tilde{b}} \\
&- \frac{1}{8\pi^2}\frac{g_{\phi 11} g_{\phi 12}}{g_{\phi bb}^2} tD_{123}(-p_1,p_3,p_4,m_{\tilde{g}},m_{\tilde{b}_2},m_{\tilde{b}_1},m_{\tilde{b}_1})\sin\theta_{\tilde{b}}\cos\theta_{\tilde{b}} \\
&+ \frac{1}{8\pi^2}\frac{g_{\phi 12}^2}{g_{\phi bb}^2} tD_{123}(-p_1,p_3,p_4,m_{\tilde{g}},m_{\tilde{b}_2},m_{\tilde{b}_1},m_{\tilde{b}_2})\sin^2\theta_{\tilde{b}} \\
&- \frac{1}{8\pi^2}\frac{g_{\phi 22} g_{\phi 12}}{g_{\phi bb}^2} tD_{123}(-p_1,p_3,p_4,m_{\tilde{g}},m_{\tilde{b}_2},m_{\tilde{b}_2},m_{\tilde{b}_1})\sin\theta_{\tilde{b}}\cos\theta_{\tilde{b}} \\
&+ \frac{1}{8\pi^2}\frac{g_{\phi 22}^2}{g_{\phi bb}^2} tD_{123}(-p_1,p_3,p_4,m_{\tilde{g}},m_{\tilde{b}_2},m_{\tilde{b}_2},m_{\tilde{b}_2})\sin^2\theta_{\tilde{b}}
\end{aligned}
$$

$$
\begin{aligned}
X_{72} &= \frac{1}{8\pi^2}\frac{g_{\phi 11}^2}{g_{\phi bb}^2} tD_{123}(-p_1,p_3,p_4,m_{\tilde{g}},m_{\tilde{b}_1},m_{\tilde{b}_1},m_{\tilde{b}_1})\sin^2\theta_{\tilde{b}} \\
&+ \frac{1}{8\pi^2}\frac{g_{\phi 11}g_{\phi 12}}{g_{\phi bb}^2} tD_{123}(-p_1,p_3,p_4,m_{\tilde{g}},m_{\tilde{b}_1},m_{\tilde{b}_1},m_{\tilde{b}_2})\sin\theta_{\tilde{b}}\cos\theta_{\tilde{b}} \\
&+ \frac{1}{8\pi^2}\frac{g_{\phi 12}^2}{g_{\phi bb}^2} tD_{123}(-p_1,p_3,p_4,m_{\tilde{g}},m_{\tilde{b}_1},m_{\tilde{b}_2},m_{\tilde{b}_1})\sin^2\theta_{\tilde{b}} \\
&+ \frac{1}{8\pi^2}\frac{g_{\phi 22}g_{\phi 12}}{g_{\phi bb}^2} tD_{123}(-p_1,p_3,p_4,m_{\tilde{g}},m_{\tilde{b}_1},m_{\tilde{b}_2},m_{\tilde{b}_2})\sin\theta_{\tilde{b}}\cos\theta_{\tilde{b}} \\
&+ \frac{1}{8\pi^2}\frac{g_{\phi 11}g_{\phi 12}}{g_{\phi bb}^2} tD_{123}(-p_1,p_3,p_4,m_{\tilde{g}},m_{\tilde{b}_2},m_{\tilde{b}_1},m_{\tilde{b}_1})\sin\theta_{\tilde{b}}\cos\theta_{\tilde{b}} \\
&+ \frac{1}{8\pi^2}\frac{g_{\phi 12}^2}{g_{\phi bb}^2} tD_{123}(-p_1,p_3,p_4,m_{\tilde{g}},m_{\tilde{b}_2},m_{\tilde{b}_1},m_{\tilde{b}_2})\cos^2\theta_{\tilde{b}} \\
&+ \frac{1}{8\pi^2}\frac{g_{\phi 22}g_{\phi 12}}{g_{\phi bb}^2} tD_{123}(-p_1,p_3,p_4,m_{\tilde{g}},m_{\tilde{b}_2},m_{\tilde{b}_2},m_{\tilde{b}_1})\sin\theta_{\tilde{b}}\cos\theta_{\tilde{b}} \\
&+ \frac{1}{8\pi^2}\frac{g_{\phi 22}^2}{g_{\phi bb}^2} tD_{123}(-p_1,p_3,p_4,m_{\tilde{g}},m_{\tilde{b}_2},m_{\tilde{b}_2},m_{\tilde{b}_2})\cos^2\theta_{\tilde{b}} \\
X_{73} &= -\frac{1}{8\pi^2} g_{\phi 11}^2 m_{\tilde{g}} D_0(-p_1,p_3,p_4,m_{\tilde{g}},m_{\tilde{b}_1},m_{\tilde{b}_1},m_{\tilde{b}_1})\sin\theta_{\tilde{b}}\cos\theta_{\tilde{b}} \\
&- \frac{1}{8\pi^2} g_{\phi 11}g_{\phi 12} m_{\tilde{g}} D_0(-p_1,p_3,p_4,m_{\tilde{g}},m_{\tilde{b}_1},m_{\tilde{b}_1},m_{\tilde{b}_2})\cos^2\theta_{\tilde{b}} \\
&- \frac{1}{8\pi^2} g_{\phi 12}^2 m_{\tilde{g}} D_0(-p_1,p_3,p_4,m_{\tilde{g}},m_{\tilde{b}_1},m_{\tilde{b}_2},m_{\tilde{b}_1})\sin\theta_{\tilde{b}}\cos\theta_{\tilde{b}} \\
&- \frac{1}{8\pi^2} g_{\phi 22}g_{\phi 12} m_{\tilde{g}} D_0(-p_1,p_3,p_4,m_{\tilde{g}},m_{\tilde{b}_1},m_{\tilde{b}_2},m_{\tilde{b}_2})\cos^2\theta_{\tilde{b}} \\
&+ \frac{1}{8\pi^2} g_{\phi 11}g_{\phi 12} m_{\tilde{g}} D_0(-p_1,p_3,p_4,m_{\tilde{g}},m_{\tilde{b}_2},m_{\tilde{b}_1},m_{\tilde{b}_1})\sin^2\theta_{\tilde{b}} \\
&+ \frac{1}{8\pi^2} g_{\phi 12}^2 m_{\tilde{g}} D_0(-p_1,p_3,p_4,m_{\tilde{g}},m_{\tilde{b}_2},m_{\tilde{b}_1},m_{\tilde{b}_2})\sin\theta_{\tilde{b}}\cos\theta_{\tilde{b}} \\
&+ \frac{1}{8\pi^2} g_{\phi 22}g_{\phi 12} m_{\tilde{g}} D_0(-p_1,p_3,p_4,m_{\tilde{g}},m_{\tilde{b}_2},m_{\tilde{b}_2},m_{\tilde{b}_1})\sin^2\theta_{\tilde{b}} \\
&+ \frac{1}{8\pi^2} g_{\phi 22}^2 m_{\tilde{g}} D_0(-p_1,p_3,p_4,m_{\tilde{g}},m_{\tilde{b}_2},m_{\tilde{b}_2},m_{\tilde{b}_2})\sin\theta_{\tilde{b}}\cos\theta_{\tilde{b}} \\
X_{74} &= -\frac{1}{8\pi^2} g_{\phi 11}^2 m_{\tilde{g}} D_0(-p_1,p_3,p_4,m_{\tilde{g}},m_{\tilde{b}_1},m_{\tilde{b}_1},m_{\tilde{b}_1})\sin\theta_{\tilde{b}}\cos\theta_{\tilde{b}} \\
&+ \frac{1}{8\pi^2} g_{\phi 11}g_{\phi 12} m_{\tilde{g}} D_0(-p_1,p_3,p_4,m_{\tilde{g}},m_{\tilde{b}_1},m_{\tilde{b}_1},m_{\tilde{b}_2})\sin^2\theta_{\tilde{b}} \\
&- \frac{1}{8\pi^2} g_{\phi 12}^2 m_{\tilde{g}} D_0(-p_1,p_3,p_4,m_{\tilde{g}},m_{\tilde{b}_1},m_{\tilde{b}_2},m_{\tilde{b}_1})\sin\theta_{\tilde{b}}\cos\theta_{\tilde{b}} \\
&+ \frac{1}{8\pi^2} g_{\phi 22}g_{\phi 12} m_{\tilde{g}} D_0(-p_1,p_3,p_4,m_{\tilde{g}},m_{\tilde{b}_1},m_{\tilde{b}_2},m_{\tilde{b}_2})\sin^2\theta_{\tilde{b}} \\
&- \frac{1}{8\pi^2} g_{\phi 11}g_{\phi 12} m_{\tilde{g}} D_0(-p_1,p_3,p_4,m_{\tilde{g}},m_{\tilde{b}_2},m_{\tilde{b}_1},m_{\tilde{b}_1})\cos^2\theta_{\tilde{b}} \\
&+ \frac{1}{8\pi^2} g_{\phi 12}^2 m_{\tilde{g}} D_0(-p_1,p_3,p_4,m_{\tilde{g}},m_{\tilde{b}_2},m_{\tilde{b}_1},m_{\tilde{b}_2})\sin\theta_{\tilde{b}}\cos\theta_{\tilde{b}}
\end{aligned}
$$

$$
\begin{aligned}
&- \frac{1}{8\pi^2} g_{\phi 22} g_{\phi 12} m_{\tilde{g}} D_0(-p_1, p_3, p_4, m_{\tilde{g}}, m_{\tilde{b}_2}, m_{\tilde{b}_2}, m_{\tilde{b}_1}) \cos^2\theta_{\tilde{b}} \\
&+ \frac{1}{8\pi^2} g_{\phi 22}^2 m_{\tilde{g}} D_0(-p_1, p_3, p_4, m_{\tilde{g}}, m_{\tilde{b}_2}, m_{\tilde{b}_2}, m_{\tilde{b}_2}) \sin\theta_{\tilde{b}} \cos\theta_{\tilde{b}}
\end{aligned}
$$

$$
X_{8i} = X_{7i}(t \leftrightarrow u, p_3 \leftrightarrow p_4) \quad i = 1, 2, 3, 4
$$

$$
\begin{aligned}
X_{93} &= -\frac{1}{8\pi^2} g_{h11} g_{h\phi\phi} \frac{m_{\tilde{g}}}{(s - M_h^2) + i M_h \Gamma_h} C_0(-p_1, p_1 + p_2, m_{\tilde{g}}, m_{\tilde{b}_1}, m_{\tilde{b}_1}) \sin\theta_{\tilde{b}} \cos\theta_{\tilde{b}} \\
&- \frac{1}{8\pi^2} g_{h12} g_{h\phi\phi} \frac{m_{\tilde{g}}}{(s - M_h^2) + i M_h \Gamma_h} C_0(-p_1, p_1 + p_2, m_{\tilde{g}}, m_{\tilde{b}_1}, m_{\tilde{b}_2}) \cos^2\theta_{\tilde{b}} \\
&+ \frac{1}{8\pi^2} g_{h12} g_{h\phi\phi} \frac{m_{\tilde{g}}}{(s - M_h^2) + i M_h \Gamma_h} C_0(-p_1, p_1 + p_2, m_{\tilde{g}}, m_{\tilde{b}_2}, m_{\tilde{b}_1}) \sin^2\theta_{\tilde{b}} \\
&+ \frac{1}{8\pi^2} g_{h22} g_{h\phi\phi} \frac{m_{\tilde{g}}}{(s - M_h^2) + i M_h \Gamma_h} C_0(-p_1, p_1 + p_2, m_{\tilde{g}}, m_{\tilde{b}_2}, m_{\tilde{b}_2}) \sin\theta_{\tilde{b}} \cos\theta_{\tilde{b}} \\
X_{94} &= -\frac{1}{8\pi^2} g_{h11} g_{h\phi\phi} \frac{m_{\tilde{g}}}{(s - M_h^2) + i M_h \Gamma_h} C_0(-p_1, p_1 + p_2, m_{\tilde{g}}, m_{\tilde{b}_1}, m_{\tilde{b}_1}) \sin\theta_{\tilde{b}} \cos\theta_{\tilde{b}} \\
&+ \frac{1}{8\pi^2} g_{h12} g_{h\phi\phi} \frac{m_{\tilde{g}}}{(s - M_h^2) + i M_h \Gamma_h} C_0(-p_1, p_1 + p_2, m_{\tilde{g}}, m_{\tilde{b}_1}, m_{\tilde{b}_2}) \sin^2\theta_{\tilde{b}} \\
&- \frac{1}{8\pi^2} g_{h12} g_{h\phi\phi} \frac{m_{\tilde{g}}}{(s - M_h^2) + i M_h \Gamma_h} C_0(-p_1, p_1 + p_2, m_{\tilde{g}}, m_{\tilde{b}_2}, m_{\tilde{b}_1}) \cos^2\theta_{\tilde{b}} \\
&+ \frac{1}{8\pi^2} g_{h22} g_{h\phi\phi} \frac{m_{\tilde{g}}}{(s - M_h^2) + i M_h \Gamma_h} C_0(-p_1, p_1 + p_2, m_{\tilde{g}}, m_{\tilde{b}_2}, m_{\tilde{b}_2}) \sin\theta_{\tilde{b}} \cos\theta_{\tilde{b}}
\end{aligned}
$$

$$
X_{10i} = X_{9i}(g_{hjk} \leftrightarrow g_{Hjk}, g_{h\phi\phi} \leftrightarrow g_{H\phi\phi}) \quad i = 3, 4; \quad j, k = 1, 2
$$

(B1)

2. X coefficients for $b\bar{b} \to AA$

$$
\begin{aligned}
X_{11} &= \frac{1}{8\pi^2} \left[B_1(-p_1 + p_3, m_{\tilde{g}}, m_{\tilde{b}_1}) \sin^2\theta_{\tilde{b}} + B_1(-p_1 + p_3, m_{\tilde{g}}, m_{\tilde{b}_2}) \cos^2\theta_{\tilde{b}} \right] \\
X_{12} &= \frac{1}{8\pi^2} \left[B_1(-p_1 + p_3, m_{\tilde{g}}, m_{\tilde{b}_1}) \cos^2\theta_{\tilde{b}} + B_1(-p_1 + p_3, m_{\tilde{g}}, m_{\tilde{b}_2}) \sin^2\theta_{\tilde{b}} \right] \\
X_{13} &= \frac{1}{8\pi^2} \frac{g_{hbb}^2}{t} m_{\tilde{g}} \left[B_0(-p_1 + p_3, m_{\tilde{g}}, m_{\tilde{b}_1}) - B_0(-p_1 + p_3, m_{\tilde{g}}, m_{\tilde{b}_2}) \right] \sin\theta_{\tilde{b}} \cos\theta_{\tilde{b}} \\
X_{14} &= X_{13}
\end{aligned}
$$

$$
X_{2i} = X_{1i}(t \leftrightarrow u, p_3 \leftrightarrow p_4) \quad i = 1, 2, 3, 4
$$

$$
X_{31} = \frac{1}{8\pi^2} \frac{g_{A12}}{g_{Abb}} m_{\tilde{g}} C_0(-p_1, p_3, m_{\tilde{g}}, m_{\tilde{b}_1}, m_{\tilde{b}_2}) \cos^2\theta_{\tilde{b}}
$$

$$
\begin{aligned}
&+ \frac{1}{8\pi^2}\frac{g_{A12}}{g_{Abb}} m_{\tilde{g}} C_0(-p_1,p_3,m_{\tilde{g}},m_{\tilde{b}_2},m_{\tilde{b}_1})\sin^2\theta_{\tilde{b}} \\
X_{32} &= \frac{1}{8\pi^2}\frac{g_{A12}}{g_{Abb}} m_{\tilde{g}} C_0(-p_1,p_3,m_{\tilde{g}},m_{\tilde{b}_1},m_{\tilde{b}_2})\sin^2\theta_{\tilde{b}} \\
&+ \frac{1}{8\pi^2}\frac{g_{A12}}{g_{Abb}} m_{\tilde{g}} C_0(-p_1,p_3,m_{\tilde{g}},m_{\tilde{b}_2},m_{\tilde{b}_1})\cos^2\theta_{\tilde{b}} \\
X_{33} &= -\frac{1}{8\pi^2} g_{Abb} g_{A12} C_{12}(-p_1,p_3,m_{\tilde{g}},m_{\tilde{b}_1},m_{\tilde{b}_2})\sin\theta_{\tilde{b}}\cos\theta_{\tilde{b}} \\
&+ \frac{1}{8\pi^2} g_{Abb} g_{A12} C_{12}(-p_1,p_3,m_{\tilde{g}},m_{\tilde{b}_2},m_{\tilde{b}_1})\sin\theta_{\tilde{b}}\cos\theta_{\tilde{b}} \\
X_{34} &= -\frac{1}{8\pi^2} g_{Abb} g_{A12} C_{12}(-p_1,p_3,m_{\tilde{g}},m_{\tilde{b}_1},m_{\tilde{b}_2})\sin\theta_{\tilde{b}}\cos\theta_{\tilde{b}} \\
&+ \frac{1}{8\pi^2} g_{Abb} g_{A12} C_{12}(-p_1,p_3,m_{\tilde{g}},m_{\tilde{b}_2},m_{\tilde{b}_1})\sin\theta_{\tilde{b}}\cos\theta_{\tilde{b}} \\
X_{4i} &= X_{3i}(t\leftrightarrow u, p_3\leftrightarrow p_4) \quad i=1,2,3,4 \\
X_{51} &= \frac{1}{8\pi^2}\frac{g_{A12}}{g_{Abb}} m_{\tilde{g}} C_0(p_2,-p_4,m_{\tilde{g}},m_{\tilde{b}_2},m_{\tilde{b}_1})\sin^2\theta_{\tilde{b}} \\
&+ \frac{1}{8\pi^2}\frac{g_{A12}}{g_{Abb}} m_{\tilde{g}} C_0(p_2,-p_4,m_{\tilde{g}},m_{\tilde{b}_1},m_{\tilde{b}_2})\cos^2\theta_{\tilde{b}} \\
X_{52} &= \frac{1}{8\pi^2}\frac{g_{A12}}{g_{Abb}} m_{\tilde{g}} C_0(p_2,-p_4,m_{\tilde{g}},m_{\tilde{b}_2},m_{\tilde{b}_1})\cos^2\theta_{\tilde{b}} \\
&+ \frac{1}{8\pi^2}\frac{g_{A12}}{g_{Abb}} m_{\tilde{g}} C_0(p_2,-p_4,m_{\tilde{g}},m_{\tilde{b}_1},m_{\tilde{b}_2})\sin^2\theta_{\tilde{b}} \\
X_{53} &= \frac{1}{8\pi^2} g_{Abb} g_{A12} C_{12}(p_2,-p_4,m_{\tilde{g}},m_{\tilde{b}_2},m_{\tilde{b}_1})\sin\theta_{\tilde{b}}\cos\theta_{\tilde{b}} \\
&- \frac{1}{8\pi^2} g_{Abb} g_{A12} C_{12}(p_2,-p_4,m_{\tilde{g}},m_{\tilde{b}_1},m_{\tilde{b}_2})\sin\theta_{\tilde{b}}\cos\theta_{\tilde{b}} \\
X_{54} &= \frac{1}{8\pi^2} g_{Abb} g_{A12} C_{12}(p_2,-p_4,m_{\tilde{g}},m_{\tilde{b}_2},m_{\tilde{b}_1})\sin\theta_{\tilde{b}}\cos\theta_{\tilde{b}} \\
&- \frac{1}{8\pi^2} g_{Abb} g_{A12} C_{12}(p_2,-p_4,m_{\tilde{g}},m_{\tilde{b}_1},m_{\tilde{b}_2})\sin\theta_{\tilde{b}}\cos\theta_{\tilde{b}} \\
X_{6i} &= X_{5i}(t\leftrightarrow u, p_3\leftrightarrow p_4) \quad i=1,2,3,4 \\
X_{71} &= \frac{1}{8\pi^2}\frac{g_{A12}^2}{g_{Abb}^2} tD_{123}(-p_1,p_3,p_4,m_{\tilde{g}},m_{\tilde{b}_1},m_{\tilde{b}_2},m_{\tilde{b}_1})\cos^2\theta_{\tilde{b}} \\
&+ \frac{1}{8\pi^2}\frac{g_{A12}^2}{g_{Abb}^2} tD_{123}(-p_1,p_3,p_4,m_{\tilde{g}},m_{\tilde{b}_2},m_{\tilde{b}_1},m_{\tilde{b}_2})\sin^2\theta_{\tilde{b}} \\
X_{72} &= \frac{1}{8\pi^2}\frac{g_{A12}^2}{g_{Abb}^2} tD_{123}(-p_1,p_3,p_4,m_{\tilde{g}},m_{\tilde{b}_1},m_{\tilde{b}_2},m_{\tilde{b}_1})\sin^2\theta_{\tilde{b}} \\
&+ \frac{1}{8\pi^2}\frac{g_{A12}^2}{g_{Abb}^2} tD_{123}(-p_1,p_3,p_4,m_{\tilde{g}},m_{\tilde{b}_2},m_{\tilde{b}_1},m_{\tilde{b}_2})\cos^2\theta_{\tilde{b}}
\end{aligned}
$$

$$
\begin{aligned}
X_{73} &= -\frac{1}{8\pi^2} g_{A12}^2 m_{\tilde{g}} D_0(-p_1, p_3, p_4, m_{\tilde{g}}, m_{\tilde{b}_1}, m_{\tilde{b}_2}, m_{\tilde{b}_1}) \sin\theta_{\tilde{b}} \cos\theta_{\tilde{b}} \\
&+ \frac{1}{8\pi^2} g_{A12}^2 m_{\tilde{g}} D_0(-p_1, p_3, p_4, m_{\tilde{g}}, m_{\tilde{b}_2}, m_{\tilde{b}_1}, m_{\tilde{b}_2}) \sin\theta_{\tilde{b}} \cos\theta_{\tilde{b}} \\
X_{74} &= -\frac{1}{8\pi^2} g_{A12}^2 m_{\tilde{g}} D_0(-p_1, p_3, p_4, m_{\tilde{g}}, m_{\tilde{b}_1}, m_{\tilde{b}_2}, m_{\tilde{b}_1}) \sin\theta_{\tilde{b}} \cos\theta_{\tilde{b}} \\
&+ \frac{1}{8\pi^2} g_{A12}^2 m_{\tilde{g}} D_0(-p_1, p_3, p_4, m_{\tilde{g}}, m_{\tilde{b}_2}, m_{\tilde{b}_1}, m_{\tilde{b}_2}) \sin\theta_{\tilde{b}} \cos\theta_{\tilde{b}} \\
X_{8i} &= X_{7i}(t \leftrightarrow u, p_3 \leftrightarrow p_4) \quad i = 1, 2, 3, 4 \\
X_{93} &= -\frac{1}{8\pi^2} g_{h11} g_{hAA} \frac{m_{\tilde{g}}}{(s - M_h^2) + iM_h\Gamma_h} C_0(-p_1, p_1 + p_2, m_{\tilde{g}}, m_{\tilde{b}_1}, m_{\tilde{b}_1}) \sin\theta_{\tilde{b}} \cos\theta_{\tilde{b}} \\
&- \frac{1}{8\pi^2} g_{h12} g_{hAA} \frac{m_{\tilde{g}}}{(s - M_h^2) + iM_h\Gamma_h} C_0(-p_1, p_1 + p_2, m_{\tilde{g}}, m_{\tilde{b}_1}, m_{\tilde{b}_2}) \cos^2\theta_{\tilde{b}} \\
&+ \frac{1}{8\pi^2} g_{h12} g_{hAA} \frac{m_{\tilde{g}}}{(s - M_h^2) + iM_h\Gamma_h} C_0(-p_1, p_1 + p_2, m_{\tilde{g}}, m_{\tilde{b}_2}, m_{\tilde{b}_1}) \sin^2\theta_{\tilde{b}} \\
&+ \frac{1}{8\pi^2} g_{h22} g_{hAA} \frac{m_{\tilde{g}}}{(s - M_h^2) + iM_h\Gamma_h} C_0(-p_1, p_1 + p_2, m_{\tilde{g}}, m_{\tilde{b}_2}, m_{\tilde{b}_2}) \sin\theta_{\tilde{b}} \cos\theta_{\tilde{b}} \\
X_{94} &= -\frac{1}{8\pi^2} g_{h11} g_{hAA} \frac{m_{\tilde{g}}}{(s - M_h^2) + iM_h\Gamma_h} C_0(-p_1, p_1 + p_2, m_{\tilde{g}}, m_{\tilde{b}_1}, m_{\tilde{b}_1}) \sin\theta_{\tilde{b}} \cos\theta_{\tilde{b}} \\
&+ \frac{1}{8\pi^2} g_{h12} g_{hAA} \frac{m_{\tilde{g}}}{(s - M_h^2) + iM_h\Gamma_h} C_0(-p_1, p_1 + p_2, m_{\tilde{g}}, m_{\tilde{b}_1}, m_{\tilde{b}_2}) \sin^2\theta_{\tilde{b}} \\
&- \frac{1}{8\pi^2} g_{h12} g_{hAA} \frac{m_{\tilde{g}}}{(s - M_h^2) + iM_h\Gamma_h} C_0(-p_1, p_1 + p_2, m_{\tilde{g}}, m_{\tilde{b}_2}, m_{\tilde{b}_1}) \cos^2\theta_{\tilde{b}} \\
&+ \frac{1}{8\pi^2} g_{h22} g_{hAA} \frac{m_{\tilde{g}}}{(s - M_h^2) + iM_h\Gamma_h} C_0(-p_1, p_1 + p_2, m_{\tilde{g}}, m_{\tilde{b}_2}, m_{\tilde{b}_2}) \sin\theta_{\tilde{b}} \cos\theta_{\tilde{b}} \\
X_{10i} &= X_{9i}(g_{hjk} \leftrightarrow g_{Hjk}, g_{hAA} \leftrightarrow g_{HAA}) \quad i = 3, 4; \quad j, k = 1, 2
\end{aligned}
\tag{B2}
$$

APPENDIX C: HIGGS COUPLINGS IN MSSM

g_{hbb}	g_{Hbb}	g_{Abb}
$\frac{gm_b}{2M_W}\frac{\sin\alpha}{\cos\beta}$	$-\frac{gm_b}{2M_W}\frac{\cos\alpha}{\cos\beta}$	$-\frac{gm_b}{2M_W}\tan\beta$

TABLE I: The $\phi b\bar{b}$ vertex couplings. For $\phi = h, H$ the Feynman rule is $ig_{\phi bb}$ and for $\phi = A$ the Feynman rule is $\gamma_5 g_{Abb}$.

g	h	H
hh	$-3\frac{gM_Z}{2\cos\theta_W}\cos 2\alpha \sin(\beta+\alpha)$	$-\frac{gM_Z}{2\cos\theta_W}[2\sin 2\alpha\sin(\beta+\alpha) - \cos(\beta+\alpha)\cos 2\alpha]$
HH	$\frac{gM_Z}{2\cos\theta_W}[2\sin 2\alpha\cos(\beta+\alpha) + \sin(\beta+\alpha)\cos 2\alpha]$	$-3\frac{gM_Z}{2\cos\theta_W}\cos 2\alpha\cos(\beta+\alpha)$
AA	$-\frac{gM_Z}{2\cos\theta_W}\cos 2\beta\sin(\beta+\alpha)$	$\frac{gM_Z}{2\cos\theta_W}\cos 2\beta\cos(\beta+\alpha)$

TABLE II: The $\phi_i\phi_j\phi_j$ triple Higgs vertices. For $\phi = h, H, A$ the Feynman rule is $ig_{\phi_i\phi_j\phi_j}$.

g_{h11}	$\frac{gm_b}{2M_W\cos\beta}[\sin 2\theta_b(\mu\cos\alpha + A_b\sin\alpha)] + \frac{gm_b^2}{M_W\cos\beta}\sin\alpha$ $-\frac{gM_W}{2}\sin(\beta+\alpha)[(1-\frac{\tan^2\theta_w}{3})\cos^2\theta_b + \frac{2}{3}\tan^2\theta_W]$
g_{h22}	$\frac{gm_b}{2M_W\cos\beta}[-\sin 2\theta_b(\mu\cos\alpha + A_b\sin\alpha)] + \frac{gm_b^2}{M_W\cos\beta}\sin\alpha$ $-\frac{gM_W}{2}\sin(\beta+\alpha)[(1-\frac{\tan^2\theta_w}{3})\sin^2\theta_b + \frac{2}{3}\tan^2\theta_W]$
g_{h12}	$\frac{gm_b}{2M_W\cos\beta}\cos 2\theta_b(\mu\cos\alpha + A_b\sin\alpha)]$ $+\frac{gM_W}{4}\sin 2\theta_b\sin(\beta+\alpha)(1-\frac{\tan^2\theta_w}{3})$
g_{H11}	$\frac{gm_b}{2M_W\cos\beta}(\sin 2\theta_b)(\mu\sin\alpha - A_b\cos\alpha)] - \frac{gm_b^2}{M_W\cos\beta}\cos\alpha$ $+\frac{gM_W}{2}\cos(\beta+\alpha)[(1-\frac{\tan^2\theta_w}{3})\cos^2\theta_b + \frac{2}{3}\tan^2\theta_W]$
g_{H22}	$-\frac{gm_b}{2M_W\cos\beta}\sin 2\theta_b(\mu\sin\alpha - A_b\cos\alpha) - \frac{gm_b^2}{M_W\cos\beta}\cos\alpha$ $+\frac{gM_W}{2}\cos(\beta+\alpha)[(1-\frac{\tan^2\theta_w}{3})\sin^2\theta_b + \frac{2}{3}\tan^2\theta_W]$
g_{H12}	$\frac{gm_b}{2M_W\cos\beta}\cos 2\theta_b(\mu\sin\alpha - A_b\cos\alpha)$ $-\frac{gM_W}{4}\sin 2\theta_b\cos(\beta+\alpha)(1-\frac{\tan^2\theta_w}{3})$
g_{A12}	$\frac{gm_b}{2M_W\cos\beta}(\mu\cos\beta + A_b\sin\beta)$
g_{A21}	$-g_{A12}$

TABLE III: Higgs-sbottom-sbottom couplings. For $\phi = h, H$ the Feynman rule is $ig_{\phi\tilde{b}_i\tilde{b}_j}$ and for $\phi = A$ the Feynman rule is $g_{A\tilde{b}_i\tilde{b}_j}$.

[1] H. P. Nilles, Phys. Rept. **110**, 1 (1984);

[2] J. F. Gunion, H. E. Haber, G. L. Kane and S. Dawson, *The Higgs Hunter's Guide* (Addison-Wesley, Menlo Park, 1990).

[3] D. A. Dicus, C. Kao and S. S. D. Willenbrock, Phys. Lett. B **203**, 457 (1988).

[4] E. W. N. Glover and J. J. van der Bij, Nucl. Phys. B **309**, 282 (1988).

[5] T. Plehn, M. Spira and P. M. Zerwas, Nucl. Phys. B **479**, 46 (1996) [Erratum-ibid. B **531**, 655 (1998)] [arXiv:hep-ph/9603205].

[6] S. Dawson, S. Dittmaier and M. Spira, Phys. Rev. D **58**, 115012 (1998) [arXiv:hep-ph/9805244].

[7] A. Belyaev, M. Drees, O. J. P. Eboli, J. K. Mizukoshi and S. F. Novaes, Phys. Rev. D **60**, 075008 (1999) [arXiv:hep-ph/9905266].

[8] A. A. Barrientos Bendezu and B. A. Kniehl, Phys. Rev. D **64**, 035006 (2001) [arXiv:hep-ph/0103018].

[9] T. Binoth, S. Karg, N. Kauer and R. Ruckl, Phys. Rev. D **74**, 113008 (2006) [arXiv:hep-ph/0608057].

[10] S. Dawson, C. Kao, Y. Wang and P. Williams, Phys. Rev. D **75**, 013007 (2007)

[arXiv:hep-ph/0610284].
[11] L. G. Jin, C. S. Li, Q. Li, J. J. Liu and R. J. Oakes, Phys. Rev. D **71**, 095004 (2005) [arXiv:hep-ph/0501279].
[12] F. Boudjema and E. Chopin, Z. Phys. C **73**, 85 (1996) [arXiv:hep-ph/9507396].
[13] A. Djouadi, W. Kilian, M. Muhlleitner and P. M. Zerwas, Eur. Phys. J. C **10**, 45 (1999) [arXiv:hep-ph/9904287].
[14] M. Muhlleitner and M. Spira, Phys. Rev. D **68**, 117701 (2003).
[15] U. Baur, T. Plehn and D. L. Rainwater, Phys. Rev. D **69**, 053004 (2004) [arXiv:hep-ph/0310056].
[16] M. Moretti, S. Moretti, F. Piccinini, R. Pittau and A. D. Polosa, JHEP **0502**, 024 (2005) [arXiv:hep-ph/0410334].
[17] Maltoni, F. and Sullivan, Z. and Willenbrock, S., Phys. Rev. D **67**, 093005 (2003) [arXiv:hep-ph/0301033].
[18] R. V. Harlander and W. B. Kilgore, Phys. Rev. D **68**, 013001 (2003) [arXiv:hep-ph/0304035].
[19] S. Dittmaier, M. Kramer, A. Muck and T. Schluter, JHEP **0703**, 114 (2007) [arXiv:hep-ph/0611353].
[20] J. Campbell *et al.*, [arXiv:hep-ph/0405302].
[21] S. Dawson, C. B. Jackson, L. Reina and D. Wackeroth, Mod. Phys. Lett. A **21**, 89 (2006) [arXiv:hep-ph/0508293].
[22] S. Dawson, C. B. Jackson, L. Reina and D. Wackeroth, Int. J. Mod. Phys. A **20**, 3353 (2005) [arXiv:hep-ph/0409345].
[23] S. Dawson, C. B. Jackson, L. Reina and D. Wackeroth, Phys. Rev. D **69**, 074027 (2004) [arXiv:hep-ph/0311067].
[24] S. Dawson, C. B. Jackson, L. Reina and D. Wackeroth, Phys. Rev. Lett. **94**, 031802 (2005) [arXiv:hep-ph/0408077].
[25] S. Dittmaier, M. Kramer and M. Spira, Phys. Rev. D **70**, 074010 (2004) [arXiv:hep-ph/0309204].
[26] S. Dawson and C. B. Jackson, arXiv:0709.4519 [hep-ph].
[27] R. M. Barnett, H. E. Haber and D. E. Soper, Nucl. Phys. B **306**, 697 (1988).
[28] F. I. Olness and W. K. Tung, Int. J. Mod. Phys. A **2**, 1413 (1987).
[29] T. Stelzer, Z. Sullivan and S. Willenbrock, Phys. Rev. D **58**, 094021 (1998) [arXiv:hep-ph/9807340].
[30] D. Dicus, T. Stelzer, Z. Sullivan and S. Willenbrock, Phys. Rev. D **59**, 094016 (1999) [arXiv:hep-ph/9811492].
[31] G. 't Hooft and M. J. G. Veltman, Nucl. Phys. B **44**, 189 (1972).
[32] G. 't Hooft and M. J. G. Veltman, Nucl. Phys. B **153**, 365 (1979).
[33] G. J. van Oldenborgh and J. A. M. Vermaseren, Z. Phys. C **46**, 425 (1990).
[34] G. J. van Oldenborgh, Comput. Phys. Commun. **66**, 1 (1991).
[35] M. A. Aivazis, J. C. Collins, F. I. Olness and W. K. Tung, Phys. Rev. D **50**, 3102 (1994) [arXiv:hep-ph/9312319].
[36] J. C. Collins, Phys. Rev. D **58**, 094002 (1998) [arXiv:hep-ph/9806259].
[37] M. Kramer, F. I. Olness and D. E. Soper, Phys. Rev. D **62**, 096007 (2000) [arXiv:hep-ph/0003035].
[38] E. Braaten and J. P. Leveille, Phys. Rev. D **22**, 715 (1980).
[39] W. Beenakker, A. Denner, W. Hollik, R. Mertig, T. Sack and D. Wackeroth, Nucl. Phys. B **411**, 343 (1994).

[40] D. M. Pierce, arXiv:hep-ph/9805497.
[41] P. Hafliger and M. Spira, Nucl. Phys. B **719**, 35 (2005) [arXiv:hep-ph/0501164].
[42] S. Berge, W. Hollik, W. M. Mosle and D. Wackeroth, "SUSY QCD one-loop effects in (un)polarized top-pair production at hadron Phys. Rev. D **76**, 034016 (2007) [arXiv:hep-ph/0703016].
[43] L. J. Hall, R. Rattazzi and U. Sarid, Phys. Rev. D **50**, 7048 (1994) [arXiv:hep-ph/9306309].
[44] M. Carena, D. Garcia, U. Nierste and C. E. M. Wagner, Nucl. Phys. B **577**, 88 (2000) [arXiv:hep-ph/9912516].
[45] J. Guasch, P. Hafliger and M. Spira, Phys. Rev. D **68**, 115001 (2003) [arXiv:hep-ph/0305101].
[46] M. S. Carena, A. Menon, R. Noriega-Papaqui, A. Szynkman and C. E. M. Wagner, Phys. Rev. D **74**, 015009 (2006) [arXiv:hep-ph/0603106].
[47] J. Pumplin, D. R. Stump, J. Huston, H. L. Lai, P. Nadolsky and W. K. Tung, JHEP **0207**, 012 (2002) [arXiv:hep-ph/0201195].
[48] W. J. Marciano, Phys. Rev. D **29**, 580 (1984).
[49] P. Nason, S. Dawson and R. K. Ellis, Nucl. Phys. B **303**, 607 (1988).
[50] J. A. M. Vermaseren, S. A. Larin and T. van Ritbergen, Phys. Lett. B **405**, 327 (1997) [arXiv:hep-ph/9703284].
[51] H. E. Haber and G. L. Kane, Phys. Rept. **117**, 75 (1985).
[52] M. Drees, R. M.Godbole and P. Roy, *Theory and Phenomenology of Sparticles : An Account of Four-diemnsional N=1 Supersymmetry in High Energy Physics* (World Scientific)
[53] H. Haer, X. Tata, *Weak Scale Supersymmetry : From Superfields to Scattering Events* (Cambridge University Press)
[54] H. Baer, M. Bisset, C. Kao and X. Tata, Phys. Rev. D **46**, 1067 (1992).
[55] H. E. Haber, M. J. Herrero, H. E. Logan, S. Penaranda, S. Rigolin and D. Temes, Phys. Rev. D **63**, 055004 (2001) [arXiv:hep-ph/0007006].